New Neogene Index Pollen and Spore Taxa from the Solimões Basin (Western Amazonia), Brazil

Authors: Rabelo Leite, Fátima Praxedes, Ferreira Da Silva-Caminha, Silane Aparecida, and D'Apolito, Carlos

Source: Palynology, 45(1) : 115-141

Published By: AASP: The Palynological Society

URL: https://doi.org/10.1080/01916122.2020.1758971

PALYNOLOGY
2021, VOL. 45, NO. 1, 115–141
https://doi.org/10.1080/01916122.2020.1758971

New Neogene index pollen and spore taxa from the Solimões Basin (Western Amazonia), Brazil

Fátima Praxedes Rabelo Leite[a,b], Silane Aparecida Ferreira da Silva-Caminha[a] and Carlos D'Apolito[a]

[a]Faculdade de Geociências, Universidade Federal de Mato Grosso, Cuiabá, MT, Brazil; [b]Instituto de Geociências, Universidade de Brasília, Campus Universitário Darcy Ribeiro ICC – Ala Central, Brasília, DF, Brazil

ABSTRACT

In western Amazonia, palynology has been the main source of chronological information for the Neogene Period. The Solimões Formation in northwestern Brazil has hundreds of meters of fine-grained rocks that have yielded rich pollen records informing on age and paleoenvironments. Here, we present new pollen data for two boreholes (1-AS-33-AM and 1-AS-37-AM) in the Solimões Basin and one outcrop (Patos) in the Acre Basin, and describe 36 new taxa (two pteridophyte spores and 34 angiosperm pollen) plus one emendation. Palynostratigraphic zonation schemes from Venezuela and Colombia were analyzed critically to provide relative ages for our sections. We found core 33AM to span pollen zones T14 (~16–14.2 Ma), T15 (14.2–12.7 Ma) and T16 (12.7–7.1 Ma) *sensu* Jaramillo et al. (2011), while core 37AM spans zones T15? and T16. We also report the widespread occurrence of *Cyatheacidites annulatus* in outcrops of the Solimões Formation, implying the existence of latest Miocene (~7 Ma) to Pliocene sedimentation and suggesting ages older than ~7 Ma for the uppermost sediments of our boreholes. Biostratigraphic relationships also indicate that *Echitricolporites mcneillyi* and *Ladakhipollenites*? *caribbiensis* cannot be used as Pliocene markers as previously assigned. The implications of these results for the palynostratigraphy and paleoenvironmental reconstructions of western Amazonia are discussed.

KEYWORDS

Solimões Formation; Miocene; palynology; biostratigraphy; Amazonia

1. Introduction

The Solimões Formation is the most detailed geological record of the Miocene orogenic pulse of the Andes (Campbell et al. 2006) and the beginning of the Amazon River (Hoorn et al. 2010, 2017) in northwestern Brazil. It can reach up to 900 m deep in the Solimões Basin and 2200 m in the Acre Basin (Maia et al. 1977; Cunha 2007), and has recently become of increased importance in biostratigraphic studies. The Cenozoic and Cretaceous oil deposits in neighboring countries (Venezuela and Colombia) have led to detailed palynostratigraphic schemes for these periods (Germeraad et al. 1968; Lorente 1986; Muller et al. 1987; Jaramillo et al. 2011). However, the depositional context of the Solimões Basin is different and the use of these published palynostratigraphic frameworks, although useful, presents differences and discrepancies (Hoorn 1993; Latrubesse et al. 2010; Silva-Caminha et al. 2010; Silveira and Souza 2015; Leite et al. 2017; Kachniasz and Silva-Caminha 2017). The increasing number of palynological studies in wells and outcrops demands testing of the palynostratigraphic zonations for the Neogene deposits of the Solimões Formation. What is more, the paleobiodiversity information accumulated from this period has helped to elucidate the origins and processes linked to the rise of the Amazon biome (Hoorn et al. 2010; Salamanca et al. 2016; Espinosa et al. 2020); thus, a sound chronological framework is paramount to understanding diversification in the region. This study describes several new species found in cored sediments of the Solimões Formation, some of which can be the basis for establishing and refining biozones in the future. We also present new palynological data from Well 1AS-37-AM and the Patos outcrop in Acre (Latrubesse et al. 2010) and reanalyze and recalibrate the age of Well 1AS-33-AM (Leite et al. 2017).

1.1. Study area

The Solimões Basin, originally called the Upper Amazon Basin, was named by Caputo (1984). It extends for 400,000 km^2 and is limited to the north by the Guiana shield, to the south by the Brazilian shield, to the east by the Purus arch and to the west by the Iquitos arch (Eiras et al. 1994) (Figure 1). The stratigraphy can be divided into two first-order sedimentary sequences, one Paleozoic, that represents the major part of the sedimentary package, and the other Mesozoic–Cenozoic (Eiras et al. 1994).

The Solimões Formation is composed by of claystones, siltstones and fine to medium clayey sandstones, with carbonate, gypsum and ferruginous concretions, and intercalations of lignites, and with invertebrate fossils, mainly

CONTACT Fátima Praxedes Rabelo Leite fprleite@gmail.com Faculdade de Geociências, Universidade Federal de Mato Grosso, Av. Fernando Corrêa, s/n Coxipó, Cuiabá-MT 78060-900, Brazil.

Supplemental data for this article can be accessed at https://doi.org/10.1080/01916122.2020.1758971.

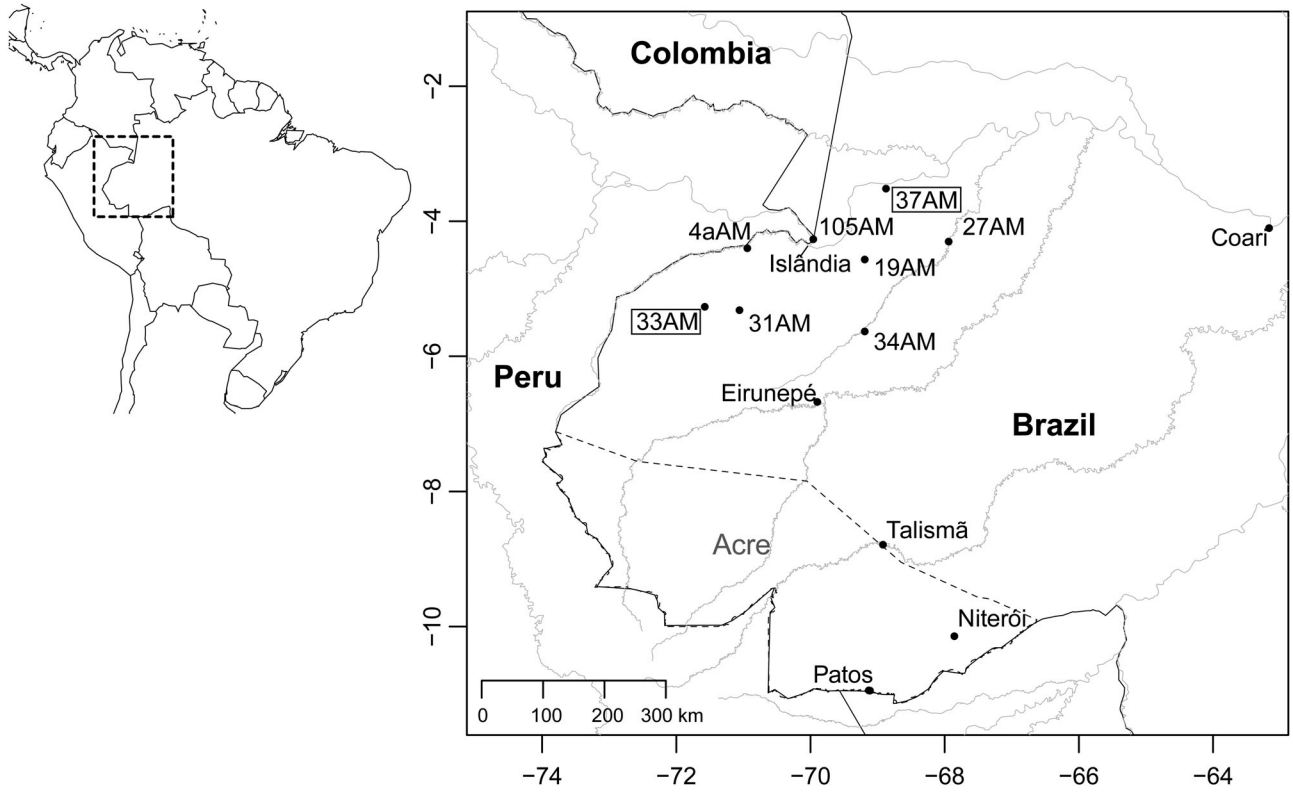

Figure 1. Study area with localities mentioned in the text. Cores: 1-AS-33-AM and 1-AS-37-AM this study; 4aAM (Hoorn 1993); 19AM and 27AM (Silva-Caminha et al. 2010); 31AM and 34AM (Kachniasz and Silva-Caminha 2017); and 105AM (Jaramillo et al. 2017). Outcrops: Coari (Nogueira et al. 2013); Islândia (Unpublished, in prep.); Eirunepé (Gross et al. 2011); Talismã and Niterói (Bissaro-Júnior et al. 2019); and Patos (this study and Latrubesse et al. 2010).

mollusks (Maia et al. 1977). The age attributed to this unit was initially Pliocene (Eiras et al. 1994); however, later studies established a Miocene age (Hoorn 1993; Latrubesse et al. 2010; Silva-Caminha et al. 2010; Silveira and Souza 2015; Jaramillo et al. 2017; Kachniasz and Silva-Caminha 2017; Leite et al. 2017; Gomes et al. 2019; Leandro et al. 2019).

The Solimões Formation has lateral continuity in neighboring basins, under different names. In the Pastaza, Marañón and Madre de Dios basins in Peru, the Neogene pelitic deposits are called the Pebas beds, Ipururo and Madre de Dios formations, respectively. In Colombia, in the Amazon and Putumayo basins, they are known as the Amazon Tertiary and La Tagua beds (Hoorn 1993; Campbell et al. 2006). In the Acre Basin, the Solimões Formation has its greatest thickness, of up to ∼2200 m (Cunha 2007). The exposed Solimões beds in these regions are well known for a rich vertebrate fauna of reptiles and mammals (Cozzuol 2006; Latrubesse et al. 2010 and references therein).

2. Materials and methods

We studied two cores from the Solimões Formation (Figures 1, 2) that were drilled by the Brazilian Geological Survey (CPRM). Core 1-AS-33-AM (hereafter 33AM) was drilled along the Curuça River, Amazonas State [5°15′S, 71°33′W; elevation 100 m above sea level (asl)] and reached a depth of 404.15 m. Core 1-AS-37-AM (hereafter 37AM) was drilled along the Jandiatuba River, Amazonas State (3°30′S, 68°51′W; 60 m asl) and reached a depth of 202.6 m. Both cores comprise the Solimões Formation except the top ∼10 m that are recent fluvial sands.

We also re-studied the palynology of the Patos outcrop in the upper Acre River (10°55′S, 69°5′20″W) (Figure 2) that had been studied by Latrubesse et al. (2007, 2010). Patos is a ∼30 m high outcrop of the Solimões Formation in a river bank cut; the lower part bears a rich vertebrate fauna (Cozzuol 2006; Latrubesse et al. 2007, 2010; and references therein) that has been dated as late Miocene by correlation with the Huayquerian South American Land Mammal Age (SALMA). Most vertebrates come from the lower conglomerate and the pollen sample from the basal clay. More slides of this stratigraphic horizon were analyzed to increase pollen counts.

The original lithological descriptions for the cores are given in Maia et al. (1977) and for the Patos outcrop in Cozzuol (2006). We entered the lithological information in Excel® sheets and constructed new columns using the package SDAR (Ortiz and Jaramillo 2019) for the R programming environment (R Core Team 2018) (Figure 2).

Sediment samples were processed for pollen recovery using standard techniques that included elimination of carbonates with hydrochloric acid (HCl), elimination of silicates with hydrofluoric acid (HF), heavy liquid separation using zinc chloride ($ZnCl_2$) at density 2 g/cm^3 and organic dissolution with potassium hydroxide (KOH). Slides were mounted with Entellan and analyzed with optical microscopes. Optical photomicrographs were made with a Leica DM750 at 1000× magnification and confocal images with a confocal laser scanning microscope (Zeiss LSM 700 confocal system).

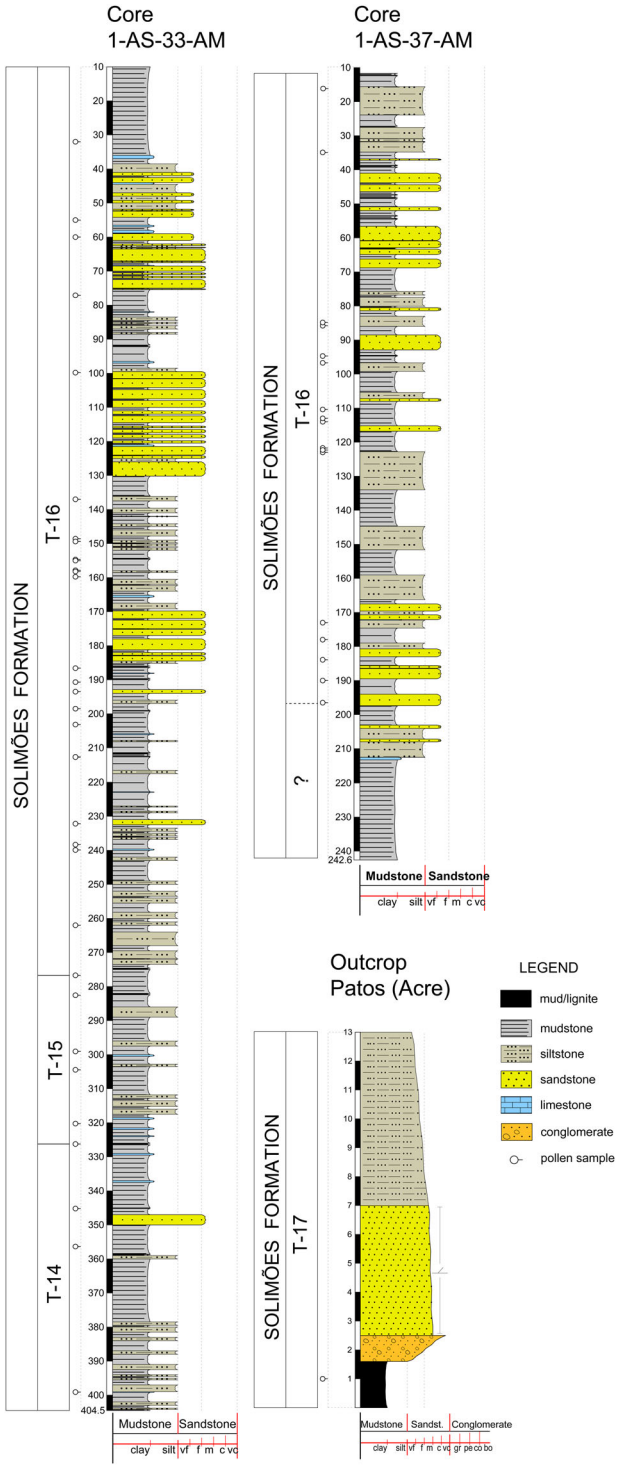

Figure 2. Lithological columns of wells 1AS-33-AM and 1AS-37-AM and outcrop Patos, western Brazilian Amazon. Pollen zones (T14–T17) after Jaramillo et al. (2011). Notice the Patos outcrop is not in the same vertical scale as the borehole sections.

Identification of pollen and spores followed South American Cenozoic palynological literature (Germeraad et al. 1968; Lorente 1986; Muller et al. 1987; Silva-Caminha et al. 2010; Jaramillo and Rueda 2020).

Palynostratigraphic markers were used to correlate cores 33AM and 37AM with existing palynological zonations. Ages for the first appearance datum (FAD) from the Llanos and Llanos Foothills Zonation (Jaramillo et al. 2011) and Venezuelan basins (Germeraad et al. 1968; Lorente 1986) were correlated with the same events from pollen data from the cores.

3. Results

3.1. Cores

A total of 32 samples from core 33AM and 17 from core 37AM were counted and yielded 30,660 palynomorphs comprising 232 different taxa (Supplementary online material), of which 36 are described as new species (two pteridophyte spores and 34 angiosperm pollen) plus one emendation. Among these, we found many key taxa used in the palynological zonations from Colombia (Jaramillo et al. 2011) and Venezuela (Germeraad et al. 1968; Lorente 1986) (Figure 3). When comparing the FAD events for these key taxa and their ages proposed in Colombia and Venezuela, a good correspondence of events can be observed (Figure 4). The bottom of core 33AM has many key taxa, but because of the edge effect (Foote 2000) those events are not reliable. However, the consistent appearance of *Crassoretitriletes vanraadshooveni* at 326.25 m (Figure 3) and the subsequent FADs of other important marker taxa such as *Fenestrites spinosus* (276.7 m), *Cichoreacidites longispinosus* (262 m), *Ladakhipollenites*? *caribbiensis* (239.9 m) and *Paleosantalaceapites cingulatus* (232.18 m) provide a consistent sequence of events. The FAD of *C. vanraadshooveni* marks the base of biozone T-15 (Jaramillo et al. 2011) at ~14.2 Ma, and the FAD of *F. spinosus* marks the base of biozone T-16 (Jaramillo et al. 2011) at 12.7 Ma. The remaining aforementioned taxa also have their FADs in zone T-16 in the zonation of Jaramillo et al. (2011). The exception is *G. magnaclavata*, which appears at 16 Ma or before (e.g. Jaramillo et al. 2017 around 18 Ma). However, in the Venezuelan sections, Lorente (1986) marked the base of biozone *G. magnaclavata* as coinciding with nannofossil zone NN7 at ~12 Ma (Backman et al. 2012) and planktonic foraminifera zone *Globorotalia fohsi lobata* (ca. 12.8 Ma after Boudagher-Fadel 2015). This age fits well with the sequence of events from the Solimões Formation cores, and therefore we adopt it as a first consistent occurrence (FCO) for *G. magnaclavata*.

The age–depth trend developed with all these events (Figure 4) points to the bottom of the core (399.1 m) being around 16 Ma, which coincides with the FAD of *Multimarginites vanderhammeni* that has an age of 15.95 according to Jaramillo et al. (2011). In the upper half of core 33AM we recorded *Echitricolporites mcneillyi* at 77.1 m. This pollen grain is used in the Colombian and Venezuelan zonation schemes to mark the onset of the Pliocene or Pleistocene, with ages from ~1.5 Ma (Jaramillo et al. 2011) to ~5.3 Ma or slightly older in the late Miocene (Germeraad et al. 1968; Lorente 1986; Muller et al. 1987), but without an age assigned. In the Solimões Formation, however, its first occurrence can be associated to the late Miocene with an age older than 7 Ma (see section 3.2). In sum, core 33AM ranges from early middle Miocene to late late Miocene (zones T-14 to T-16 *sensu* Jaramillo et al. 2011) (Figure 4).

Core 37AM has a similar set of FAD events starting around 200 m, indicating an age in zone T-16. There are no samples

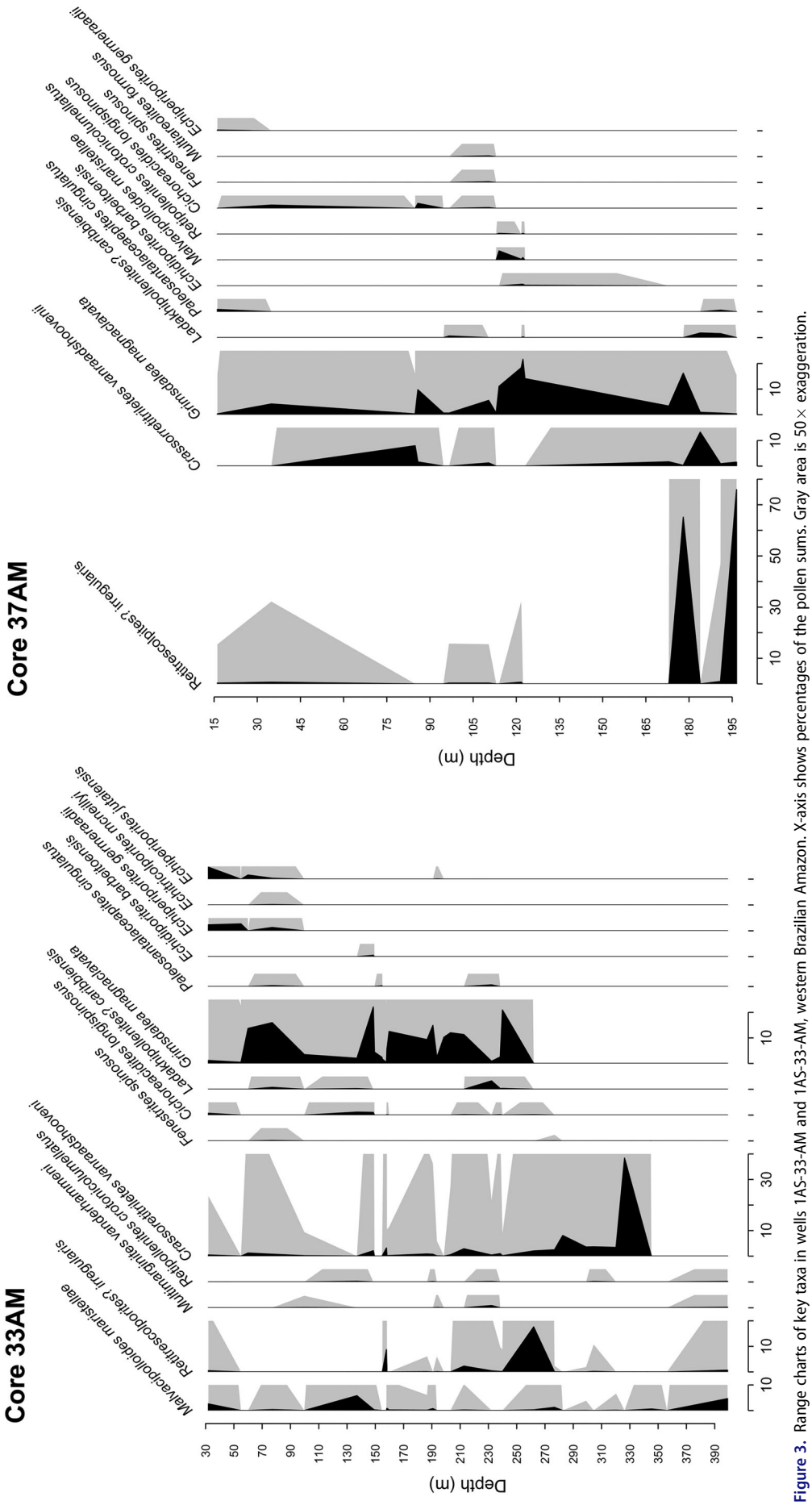

Figure 3. Range charts of key taxa in wells 1AS-33-AM and 1AS-33-AM, western Brazilian Amazon. X-axis shows percentages of the pollen sums. Gray area is 50× exaggeration.

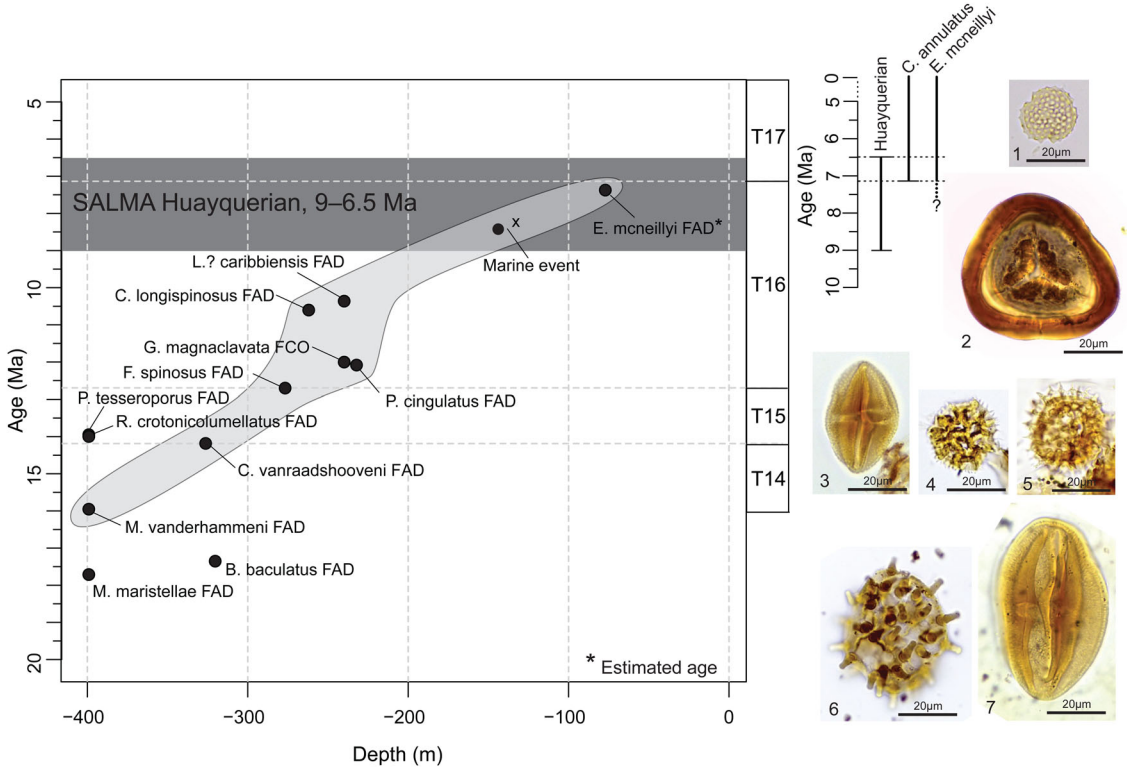

Figure 4. Comparison of events from core 1AS-33-AM against ages for key taxa suggested by Jaramillo et al. (2011) and Lorente (1986). The age–depth trend is based on first appearance datum (FAD) and first consistent occurrence (FCO) events (see text). Key taxa from the Patos outcrop are also shown (top right ranges). Gray area is the extent of the Huayquerian South American Land Mammal Age (SALMA) used to calibrate a maximum age for the FAD of *E. mcneillyi*. T14 to T17 are pollen zones from Jaramillo et al. (2011). Marine event is based on Medeiros et al. (2017, 2019) (see text). Biostratigraphic markers: 1. *Echitricolporites mcneillyi*: slide 33/77.10(6) EF W57/1; 2.*Cyatheacidites annulatus*: slide Patos 2 EF R19; 3. *Paleosantalaceapites cingulatus*: slide 33/232.18(1) EF G49/4;4. *Fenestrites spinosus*: slide 33/77.10(5) EF S33/1; 5. *Cichoreacidites longispinosus*: slide 33/137(1) EF Q53/4; 6. *Grimsdalea magnaclavata*: slide 33/239.90(2) EF H21/2-4; 7. *Ladahkipollenites*? *caribbiensis*: slide 33/238.33(3) EF J47/1.

from the bottom ~40 m. The upper half of core 37AM lacks key taxa, but a graphic correlation of cores 33AM and 37AM suggests almost all of core 37AM is correlated with the upper section (~260 m) of core 33AM (Figure 5). This comparison showed a potential correlation point in the upper section established by *Echidiporites barbeitoensis*, which in Venezuela (Falcon Basin) can be associated with the base of the Asteraceae zone (*sensu* Lorente 1986; nannofossil zone NN9 at ~10.5 Ma), in agreement with the upper sections belonging to zone T-16 (Figure 4). Furthermore, a congruent acme event of *Retitrescolpites*? *irregularis* is observed at the base of 37AM and mid-section in 33AM (Figure 3), also in agreement with the overall set of events. Finally, the topmost parts of both cores are correlated with *Echiperiporites germeraadii* sp. nov., although the validity of this event still needs to be investigated.

3.2. Patos

The Patos outcrop in the Acre region yielded 625 palynomorphs distributed in 62 taxa (Supplementary online material). A novel co-occurrence was recorded between *E. mcneillyi* and *Cyatheacidites annulatus*. The spore *C. annulatus* marks the base of zone T-17 in Jaramillo et al. (2011), at 7.15 Ma. In Venezuela, Lorente (1986) also recorded *C. annulatus* in the late Miocene *Fenestrites* sub-zone. This occurrence constrains the Patos outcrop as not older than ~7 Ma, which falls in the range of the Huayquerian SALMA biozone (9 to 6.5 Ma) that was previously applied to the outcrop (Latrubesse et al. 2007, 2010).

A new outcrop locality (Islândia; 4°21′20′S, 70°2′18″W; Figure 1) near Tabatinga contains *C. annulatus* (unpublished results; in prep.). This outcrop is just ~20 km distant from core 105AM, studied by Jaramillo et al. (2017) who also recorded *E. mcneillyi* in the core samples. This suggests a lower stratigraphic appearance of *E. mcneillyi* when compared to *C. annulatus*. Although we cannot yet establish a precise FAD age for *E. mcneillyi* for the Solimões Formation, it is logical to assume this age is older than the FAD of *C. annulatus* – 7.1 Ma (Jaramillo et al. 2011).

4. Discussion

4.1. Palynostratigraphy

The ages obtained for cores 33AM and 37AM are largely in agreement with existing biostratigraphic data for the Solimões Formation (Miocene–Pliocene). Some previously studied cores included older basal ages of early Miocene (Hoorn 1993; Jaramillo et al. 2017), while other cores are entirely middle to late Miocene (Silva-Caminha et al. 2010; Kachniasz and Silva-Caminha 2017). Hoorn (1993) applied the Venezuelan zonation of Lorente (1986) to the Solimões Formation and observed a similar sequence of events that

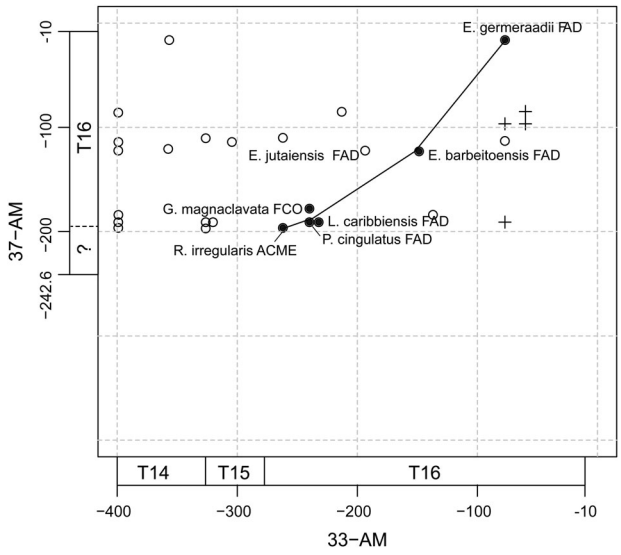

Figure 5. Graphic correlation of events from wells 1AS-33-AM and 1AS-37-AM, western Brazilian Amazon. Events are first appearance datum (FAD, circles) and last appearance datum (LAD, crosses); solid circles are events used for the line of correlation. T14 to T17 are pollen zones from Jaramillo et al. (2011).

allowed the use of key taxa for western Amazonia. Jaramillo et al. (2011) proposed an updated zonation for the Colombian Llanos that has also been successfully applied to western Amazonia (e.g. Boonstra et al. 2015; Jaramillo et al. 2017). However, it presents the FAD of *G. magnaclavata* as older than that of *C. vanraadshooveni*, marking the middle Miocene (~16 Ma). This one key event is inverted in relation to previous zonation schemes where this event is younger (late middle Miocene ~12–13 Ma). In all Solimões Formation cores studied so far (Hoorn 1993; Silva-Caminha et al. 2010; Kachniasz and Silva-Caminha 2017; Leite et al. 2017, present study), *C. vanraadshooveni* consistently appears first, agreeing with events in Venezuela (Germeraad et al. 1968; Lorente 1986). Furthermore, many key taxa, such as *C. longispinosus*, *P. cingulatus*, *F. spinosus* and *L.*? *caribbiensis*, appear synchronously with *G. magnaclavata* in the Solimões cores (Figures 3, 4), and their ages are latest middle Miocene to early late Miocene, ~10 to ~12 Ma (Jaramillo et al. 2011). We propose the use of the appearance of G. magnaclavata in core 33AM as a late middle Miocene event (~12 Ma; see Results section 3.1); the discrepancy with older ages for this taxon could be due to environmental controls or incomplete sampling, which would indicate a difference between the FAD and FCO. When using the FCO of G. magnaclavata event, the discrepancy between the *G. magnaclavata* and *C. vanraadshooveni* sequences from the Llanos (Jaramillo et al. 2011) and Venezuelan basins (Germeraad et al. 1968; Lorente 1986) is reconciled.

The upper parts of the cores are more difficult to correlate chronologically due to the lack of key taxa. However, the occurrence of *E. mcneillyi* suggests a latest Miocene age older than ~7 Ma. Critical for the establishment of this age was the co-occurrence of *E. mcneillyi* with *C. annulatus* in the Patos outcrop in Acre and the fact that *E. mcneillyi* appears consistently in core samples below outcrops. *Cyatheacidites annulatus* has never been found in samples from cores, but is widespread in outcrops of the Solimões Basin in western and central Amazonia (this study; Gross et al. 2011; Nogueira et al. 2013), spanning over 1000 km. This means that the topmost Solimões Formation is in the T-17 pollen zone, latest Miocene to Pliocene (Jaramillo et al. 2011). Leite et al. (2017) established a Pliocene age for the upper half of 33AM due to the presence of *L.*? *caribbiensis*, which is correlated to the nannofossil biozones NN12–NN15 (5.6–3.7 Ma) in Lorente (1986). However, in the present study we repositioned this interval in zone T-16 (Jaramillo et al. 2011) as it is stratigraphically below the outcrops. This configuration also indicates that the use of *L.*? *caribbiensis* as a Pliocene marker (*sensu* Lorente 1986) is invalid for the Solimões Formation.

A recent finding of detrital zircon grains in two outcrops in Acre allowed a uranium–lead (U-Pb) chronology (Bissaro-Júnior et al. 2019). The Talismã and Niterói outcrops (Figure 1) had U-Pb zircon ages of 10.89 ± 0.13 Ma and 8.5 ± 0.5 Ma, respectively, indicating maximum deposition ages. Niterói is closer to Patos (Figure 1) and both crop out on the Acre River. Although a precise stratigraphic correlation cannot be established yet due to the lack of regional mapping and structural data, this zircon age (~8 Ma) and the pollen zone of the Patos outcrop (~7 Ma) allow us to compare them chronologically to Niteroi despite the distance. Both suggest a maximum age of latest Miocene for the exposed strata of the Solimões Formation in the region.

4.2. Paleoenvironments

Core 33AM was divided into two main paleoenvironments by Leite et al. (2017). The bottom part, until 239.9 m, is predominantly a fine-grained sequence (Figure 2) accumulated in low-energy environments dominated by *Mauritiidites*, which is fossil pollen of *Mauritia* L., a palm tree adapted to permanently waterlogged environments. This environment developed in the Pebas System (Wesselingh et al. 2002; Hoorn et al. 2010) of lakes and mega-lakes. The upper section of core 33AM and almost all of core 37AM are characterized by thicker packages of sand (Figure 2) that accumulated in a more fluvial context, therefore of higher energy when compared to the lower phase. The change is also evidenced in 33AM by a significant increase in pollen diversity and compositional change (Leite et al. 2017) as well as electric logging (Jorge et al. 2019). Provenance data from core 33AM (Horbe et al. 2019) also support a change from the lower section (~400 to 287 m) to the upper section's heavy mineral and strontium/neodymium (Sr/Nd) isotopic record, which was associated to the uplift of the Eastern Peruvian Cordillera, between 25 and 10 Ma (Sundell et al. 2019), and with an orogenic peak around 12 Ma (Hoorn et al. 2010). These data corroborate the large-scale paleogeographic and drainage shifts that happened at the end of the Pebas phase (23 to 10 Ma) and beginning of the Acre Phase (10 to 7 Ma) (Hoorn et al. 2010).

Short marine inundations were recorded during the deposition of the Solimões Formation (Hoorn 1993; Boonstra et al. 2015; Jaramillo et al. 2017; Linhares et al. 2017; Sá et al. 2020).

Two marine incursions in cores 105AM (Jaramillo et al. 2017) and 4aAM (Hoorn 1993) are dated as early and middle Miocene, respectively. Linhares et al. (2017) described three marine events (early, middle and late Miocene). Although we could not find palynomorphs such as dinoflagellate cysts and foraminifera linings, Medeiros et al. (2017, 2019) studied core 33AM and found a peak of foraminifera plus coral remains and bryozoans between 139.4 and 136.35 m, comprising the late Miocene zone T-16 (Figure 4). There is also evidence of a late Miocene minor marine event by the presence of foraminifera in core 31AM (Linhares et al. 2011; Kachniasz and Silva-Caminha 2017) and ostracods in 8AM/7DAM (Linhares et al. 2019). Around 2% marine palynomorphs were reported in the Llanos Basin of Colombia around 7 Ma (Jaramillo et al. 2017), which provides a possible explanation for the origin of the flooding. The observed marine influence could also be relictual and therefore may not necessarily invoke an active connection to the Llanos. More data are needed to better constrain this event and its origins.

5. Systematic palynology

In this section we describe and illustrate new species and provide new descriptions for two published species. Taxonomy follows the latest International Code of Nomenclature for algae, fungi and plants (Turland et al. 2018). For descriptions we adopted the terminology of Punt et al. (2007) with modifications from Jaramillo and Dilcher (2001), namely the use of MLI [monolete index: laesura length/spore length] and TLI [trilete index: radius length/(spore diameter/2)]. The number observed (no) and number measured (nm) are given; we aimed to measure five specimens when available. Measurements are presented as minimum–(mean)–maximum. All measurements are provided in a supplemental digital file. Types are located using the England Finder (EF) system. All stratigraphic ranges presented are related to the cores studied herein. Some botanical affinities are offered; they were established after comparison with neotropical palynology works and the reference pollen collection of the Universidade Federal de Mato Grosso. Slides are deposited at the Paleontology and Palynology Laboratory (PALMA) of the Universidade Federal de Mato Grosso, Cuiabá (Brazil), and at the Micropaleontology Laboratory (LABMICRO), Universidade de Brasília, Brasília (Brazil).[1]

SPORES

MONOLETES

POLYPODIISPORITES Potonié 1956 emend. Khan & Martin 1972

Type species. *Polypodiisporites favus* Potonié 1956.

Polypodiisporites minutiverrucatus sp. nov.
Plate 1, figures 1–2

Holotype. 1AS-33-AM, 232.18 m (1), EF: G46/3.
Etymology. After the small, verrucate ornamentation.
Diagnosis. Monolete, mid-sized, verrucae very short and closely spaced.
Description. Monolete spore, bilateral symmetry, reniform, monolete mark distinct, curvature absent, laesura short, 21 μm long, simple, sporoderm 1 μm thick, verrucate over the whole grain, verruca 1–2 μm wide, very short, 0.5 μm tall, closely spaced ca. 0.5 μm apart.
Dimensions. Polar view length: 48 μm, width 38 μm, MLI: 0.43 (holotype); nm = 1, no = 1.
Comparisons. *Polypodiisporites usmensis* (Van der Hammen 1956a) Khan & Martin 1972 is also gemmate. *Polypodiisporites scabraproximatus* Silva-Caminha et al. (2010) has proximal face scabrate. *Polypodiisporites minutus* (Couper 1960) Khan & Martin 1971 emend. Pocknall & Mildenhall 1984 has wider and more closely spaced verrucae. *Polypodiisporites* aff. *specious* Sah 1967 is laevigate on the proximal face and the verrucae are irregular in shape and size. *Polypodiisporites pachyexinatus* Jaramillo & Dilcher (2001) has thicker sporoderm.
Stratigraphic range. T16.

TRILETES

PSILATRILETES Van der Hammen 1954 ex Potonié 1956

Type species. *Psilatriletes detortus* (Weyland & Krieger 1953) Potonié 1956.

Psilatriletes cozzuolii sp. nov.
Plate 1, figures 3–5

Holotype. 1AS-33-AM, 399,10 m (1), EF: P-36.
Paratype. 1AS-33-AM, 137 m (1), EF: S-59/2-4.
Etymology. After the Argentinian paleontologist Mario Cozzuol.
Diagnosis. Trilete, circular, large-sized, laevigate, trilete mark very small in relation to spore size.
Description. Trilete spore, radial symmetry, circular, trilete mark distinct, curvatura absent, radii very short, 20 μm long, marginate, margo 5 μm thick, thinning toward laesura ends, laevigate, sporoderm 4 μm thick.
Dimensions. Polar view length 60–(67)–74 μm, width 58–(63)–68 μm (holotype = 60 × 58 μm, paratype = 74 × 68 μm); TLI 0.12–(0.14)–0.16; nm = 2, no = 2.
Comparisons. *Deltoidospora psilostoma* Rouse 1959 is smaller and has a different shape. *Deltoidospora australis* (Couper 1953) Pocock 1970 has a triangular shape. *Leiotriletes guaduensis* (Van der Hammen 1954) Sole de Porta 1971 is smaller and has a fold on the laesura. *Leiotriletes microadriennis* Krutzsch 1959 is smaller (32–46) and the trilete mark is longer. *Matonisporites silvai* de Lima 1979 has a circular to triangular-obtuse-convex shape. *Todisporites major* Couper 1958 has longer marks.
Stratigraphic range. T14–T16.

POLLEN

INAPERTURATE

CROTONOIDAEPOLLENITES Rao & Ramanujam 1982

[1]Author names with publication year are provided for genera and species, but not listed in the references.

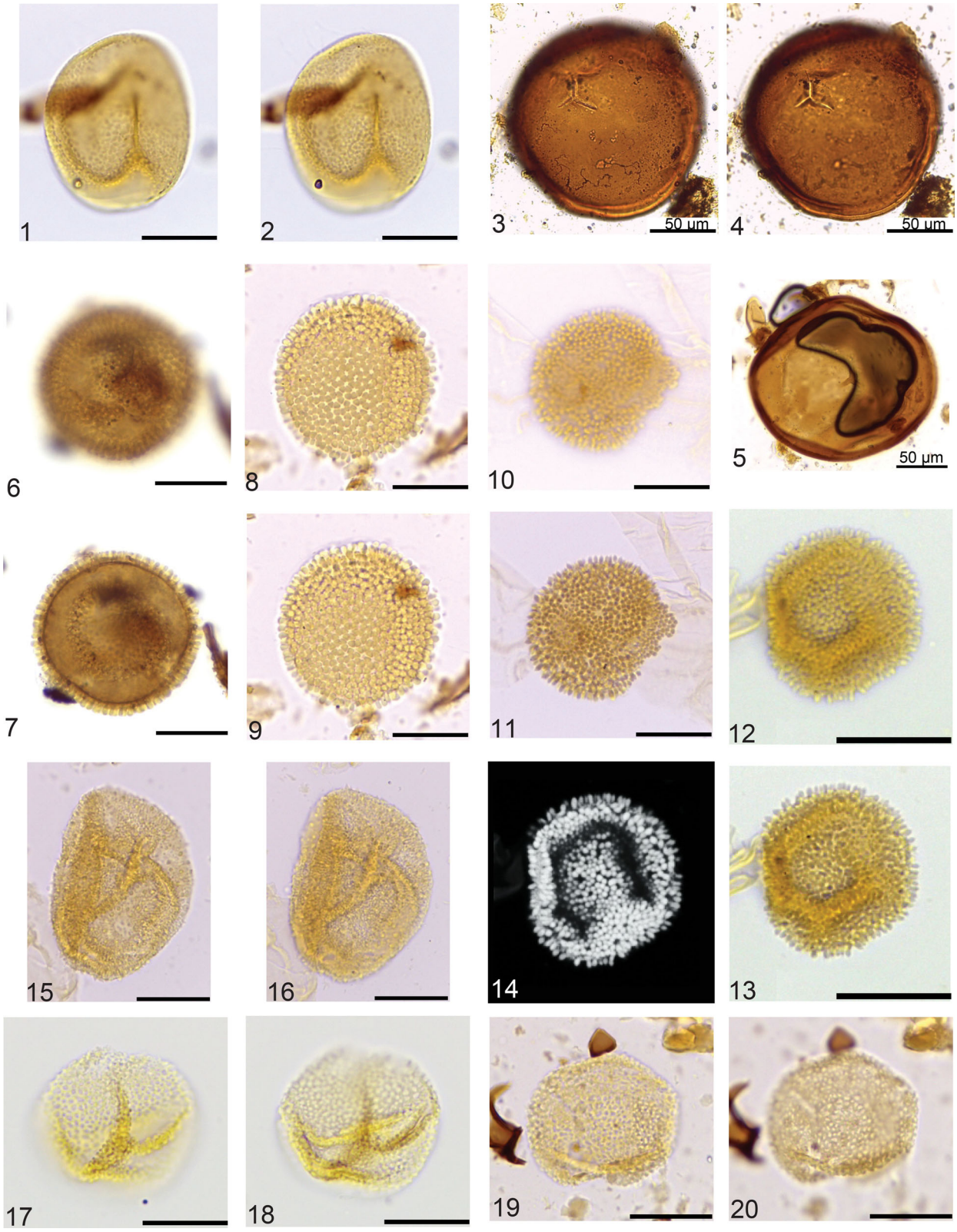

Plate 1. Figures 1, 2. *Polypodiisporites minutiverrucatus* sp. nov., holotype, 1AS-33-AM, 232.18 m (1), EF: G46/3. Figures 3, 4. *Psilatriletes cozzuolii* sp. nov., holotype, 1AS-33-AM, 399,10 m (1), EF: P-36. Figure 5. *Psilatriletes cozzuolii* sp. nov., paratype, 1AS-33-AM, 137 m (1), EF: S-59/2-4. Figures 6, 7. *Crotonoidaepollenites reticulatus* (Silva-Caminha et al. 2010) emend. holotype, AM19-1, EF: J33/3. Figures 8, 9. *Crotonoidaepollenites reticulatus* (Silva-Caminha et al. 2010) emend. 1AS-33-AM, 232.18 m (2), EF: G41/1-2. Figures 10, 11. *Crotonoidaepollenites echinatus* sp. nov., holotype, 1AS-33-AM, 154.70 m (3), EF: O24/4. Figures 12, 13, 14. *Crotonoidaepollenites echinatus* sp. nov., paratype, 1AS-33-AM, 193 m (5), EF: J37. Figures 15, 16. *Inaperturopollenites microechinatus* sp. nov., holotype, 1AS-37-AM, 114 m (3), EF: E56/4. Figures 17, 18. *Retipollenites solimoensis* sp. nov., holotype, 1AS-37-AM, 123 m (1), EF: D27/4. Figures 19, 20. *Retipollenites solimoensis* sp. nov., paratype, 1AS-33-AM, 304.45 m (1), EF: H53-J. Scale bars: 20 µm, unless otherwise noted.

Type species. *Crotonoidaepollenites euphorbioides* Rao & Ramanujam 1982.

Crotonoidaepollenites reticulatus Silva-Caminha et al. 2010
Plate 1, figures 6–9

Specimen. 1AS-33-AM, 232.18 m (2), EF: G41/1-2.
Description. Monad, radial symmetry, isopolar, circular; inaperturate; intectate, nexine 0.5–1 μm thick; sculpture clavate, clavae 3 μm tall, base 0.5 μm wide, clavae tips 1–1.5 μm wide; clavae disposed in crottonoid pattern.
Dimensions. Diameter 30–(40)–45 μm wide × 28–(37.2)–42 μm long (holotype = 45 × 42 μm, paratype = 40 × 38 μm); nm = 5, no = 79.
Remarks. The nexine was described originally as reticulate; however, some specimens do not have reticulum or it is not distinct.
Stratigraphic range. T14–T16.

Crotonoidaepollenites echinatus sp. nov.
Plate 1, figures 10–14

Holotype. 1AS-33-AM, 154.70 m (3), EF: O24/4.
Paratype. 1AS-33-AM, 193 m (5), EF: J37.
Etymology. After the clavate/echinate ornamentation.
Diagnosis. Monad, spheroidal, mid-sized, inaperturate, intectate, clavate with croton pattern ornamentation, clavae with acute top forming echinae.
Description. Monad pollen grain; spheroidal; inaperturate; intectate, nexine 1 μm; sculpture clavate/echinate, clavae arranged in crotonoid pattern; clavae 2 μm tall, base 0.8 μm wide, middle part 1.2 μm wide, top of the clavae (capita) ending in an acute point, thus resembling spines.
Dimensions. Diameter 34–(36)–40 μm long × 25–(30.4)–35 μm wide (holotype = 39 × 35 μm, paratype = 31 × 27 μm); nm = 5, no = 7.
Comparisons. *Crotonoidaepollenites reticulatus* Silva-Caminha et al. (2010) is larger and has the top of clavae rounded or flat. *Clavainaperturites clavatus* Van der Hammen & Wymstra 1964 has smaller clavae (1 μm) with a different shape. *Clavainaperturites microclavatus* Hoorn 1994 is smaller and the tectum is perforate. *Crotonoidaepollenites euphorbioides* Rao & Ramanujam 1982 is tectate.
Stratigraphic range. T16.

INAPERTUROPOLLENITES (Pflug) Potonié 1958

Type species. *Inaperturopollenites dubius* (Potonié & Venitz) Thomson & Pflug 1953.

Inaperturopollenites microechinatus sp. nov.
Plate 1, figures 15–16

Holotype. 1AS-37-AM, 114 m (3), EF: E56/4.
Etymology. After its delicate echinate ornamentation.
Diagnosis. Monad, subspheroidal, large-sized, inaperturate, tectate, echinate, echinae size <1 μm.
Description. Monad; subspheroidal; inaperturate; tectate, exine 1.7 μm, nexine 0.5 μm thick, columellae 0.8 μm tall, tectum 0.4 μm thick; sculpture echinate, echinae 0.5–1.0 μm tall, 0.5–1.0 μm wide, 2 μm apart, conical, acute, spines evenly distributed over entire grain, shadow of the columellae visible underneath the tectum, which gives the impression of a microreticulate pattern.
Dimensions. Diameter 53 μm long × 38 μm wide; nm = 1, no = 2.
Comparisons. *Cristaeturites cristatus* (van Hoeken-Klinkenberg 1964) Schrank 1994 has larger echinae. *Droseridites senonicus* Jardine & Magloire 1965 is smaller (12–24 μm) and usually found in tetrads.
Stratigraphic range. T16.

RETIPOLLENITES Gonzalez-Guzman 1967

Type species. *Retipollenites confusus* González-Guzmán 1967.

Retipollenites solimoensis sp. nov.
Plate 1, figures 17–20

Holotype. 1AS-37-AM, 123 m (1), EF: D27/4.
Paratype. 1AS-33-AM, 304.45 m (1), EF: H53-J.
Etymology. After the Solimões River.
Diagnosis. Monad, spheroidal, mid-sized, inaperturate, semitectate, reticulate, homobrochate.
Description. Monad; spheroidal; inaperturate; semitectate, exine 1 μm; tectum 0.5 μm; columellae 0.2 μm; nexine 0.3 μm; sculpture reticulate, homobrochate; lumina polygonal to rounded; lumina 0.5 μm wide; muri 1 μm, simplicolumellate; occasionally colpi-like ruptures of the exine appear, giving the grain a colpate appearance.
Dimensions. Diameter 33–(37)–40 μm long × 29–(33)–35 μm wide (holotype = 39 × 35 μm, paratype = 33 × 38 μm); nm = 5, no = 124.
Comparisons. *Inaperturopollenites cursis* Sarmiento 1992 is smaller and oblate. *Inaperturopollenites curvimuratus* Regali et al. 1974 has curvimurate reticulum.
Stratigraphic range. T14–T16.

MONOPORATE

MONOPOROPOLLENITES (Meyer 1956) Potonié 1960

Type species. *Monoporopollenites gramineoides* Meyer 1956.

Monoporopollenites scabratus sp. nov.
Plate 2, figures 1–4

Holotype. 1AS-33-AM, 203.15 m (2), EF: C30.
Paratype. 1AS-33-AM, 203.15 m (2), EF: Q44/4.
Etymology. After the scabrate ornamentation.
Diagnosis. Monad, circular, mid-sized, monoporate, tectate, scabrate and micro-foveolate.
Description. Monad pollen grain, amb circular; monoporate; tectate, exine 1.2 μm thick, nexine 0.7 μm thick, columellae indistinct, tectum 0.5 μm thick, sculpture scabrate and microfoveolate; pore circular, 4 μm wide, annulate, annulus 2 μm thick.

Dimensions. Diameter 20–(25)–30 μm long × 18–(23)–27 μm wide (holotype = 27 × 22 μm, paratype = 24 × 22 μm); nm = 5, no = 71.
Comparisons. *Monoporopollenites annulatus* (Van der Hammen) Jaramillo & Dilcher (2001) is psilate and exine is thinner. *Monoporites parcus* Sarmiento 1992 is psilate and has a simple pore.
Botanical affinity. Poaceae.
Stratigraphic range. T16.

TRIPORATE

ECHITRIPORITES (Van der Hammen 1956) Van Hoeken-Klinkenberg 1964

Type species. *Echitriporites trianguliformis* Van Hoeken-Klinkenberg 1964.

Echitriporites jolyi sp. nov.
Plate 2, figures 5–8

Holotype. 1AS-33-AM, 232.18 m (1), EF: P55/3.
Paratype. 1AS-33-AM, 232.18 m (1), EF: H41/3-J.
Etymology. After the Brazilian botanist Aylthon Brandão Joly.
Diagnosis. Monad, spheroidal, large-sized, triporate, intectate, echinate.
Description. Monad; spheroidal; triporate; intectate; nexine 0.7; sculpture echinate; tips of echinae acute; echinae 2–3 μm tall, 1–1.5 μm wide at base; evenly distributed 5 μm apart; interspine surface psilate; pore 5 μm wide, circular, faintly annulate; annulus 2 μm wide.
Dimensions. Equatorial view diameter 34–(45.6)–52 μm long × 32–(34.6)–37 μm wide (holotype = 51 × 37 μm, paratype = 35 × 52 μm (incomplete)); nm = 3, no = 3.
Comparisons. *Echitriporites nuriae* Dueñas 1980 has longer echinae (6 μm). *Echitriporites trianguliformis* var. *orbicularis* Jaramillo & Dilcher (2001) has smaller size and spines. *Bacutriporites echinatus* Jaramillo & Dilcher (2001) has echinate-baculate ornamentation.
Botanical affinity. *Cayaponia* (Cucurbitaceae).
Stratigraphic range. T16.

RETITRIPORITES Ramanujam 1966

Type species. *Retitriporites curvimurati* Ramanujam 1966.

Retitriporites crassoreticulatus sp. nov.
Plate 2, figures 9–13

Holotype. 1AS-33-AM, 239.90 m (2), EF: W47/3.
Paratype. 1AS-33-AM, 239.90 m (2), EF: X33/1.
Etymology. After the coarse reticulate ornamentation.
Diagnosis. Monad, oblate, subtriangulate, mid-sized, triporate, semitectate, reticulate, homobrochate.
Description. Monad; oblate; amb subtriangular; triporate; semitectate, nexine 0.8 μm, simplicolumellate; columella 0.8 μm tall, 1 μm wide; tectum 0.8 μm; sculpture reticulate; homobrochate; lumina irregular in shape, variable in size 2–7 μm, circular; muri 1.5 μm wide; pore 3–5 μm wide, circular, costate, costae 3 μm wide, 3 μm thick.
Dimensions. Polar view diameter 31–(33)–35 μm long × 23–(27)–31 μm wide (holotype = 31 × 31 μm, paratype= 23 × 35 μm); nm = 2, no = 2.
Comparisons. *Retitriporites* sp. 1 Silva-Caminha et al. (2010) is curvimurate and has smaller pores. *Retitriporites acostai* Duenas 1986 is heterobrochate with lumina increasing toward equator. *Rugulatitriporites vestibulipori* Muller 1968 is finely reticulate. *Retitriporites variabilis* Muller 1968 has wider lumina. *Retitriporites boltenhagenii* Salard-Cheboldaeff 1978 is smaller and has a thick annulus (3.5 μm).
Stratigraphic range. T16.

PERIPORATE

ECHIPERIPORITES (Van der Hammen & Wymstra 1964) Anzótegui 1990

Type species. *Echiperiporites akanthos* Van der Hammen & Wijmstra 1964.

Echiperiporites germeraadii sp. nov.
Plate 2, figures 14–17
Echiperiporites estelae Silva-Caminha et al. (2010), p. 71, pl. 4, figs 22–24.

Holotype. 1AS-33-AM, 77.10 m (4), EF: N27/1.
Paratype. 1AS-33-AM, 193.50 m (5), EF: J29.
Etymology. After the Dutch palynologist Johan Henri Germeraad.
Diagnosis. Monad, spheroidal, large-sized, periporate, 15 pores, annulate, tectate, echinate, size of echinae 2.5 μm.
Description. Monad pollen grain, spheroidal; periporate; 15 pores; tectate, nexine 0.8 μm, columellae 0.2 μm tall all over the grain; tectum 0.2 μm, smooth, tips of columellae distinct; sculpture echinate; echinae conical, tips acute; echinae 2.5 μm tall, 2 μm wide at base, evenly distributed 3–5 μm apart; pore 3–4 μm wide, circular, annulate, annuli 2 μm wide, 2 μm thick.
Dimensions. Diameter 44–(48.4)–54 μm long × 36–(44)–51 μm wide (holotype = 54 × 51 μm, paratype = 44 × 36 μm); nm = 5, no = 30.
Comparisons. *Echiperiporites estelae* Germeraad et al. (1968) (Plate 3, figures 5–6) has 20 or more pores, echinae 6–9 μm tall, echinae tips rounded, tectum thicker underneath spines. *Echiperiporites jutaiensis* Silva-Caminha et al. (2010) (Plate 3, figures 7–8) is smaller (28–30 μm), and has 7–11 pores and a thicker nexine. *Echiperiporites lophatus* (Plate 3, figures 9–13) Silva-Caminha et al. (2010) has lophae. *Echiperiporites jaramilloi* sp. nov. and *E. titanicus* sp. nov. are much larger in size, have larger echinae and have more pores (>20).
Stratigraphic range. T16.

Echiperiporites lophatus (Silva Caminha, Jaramillo, & Absy 2010) emend.
Plate 3, figures 1–5

Paratype. 1AS-33-AM, 77.10 m (4), EF: X35 2.

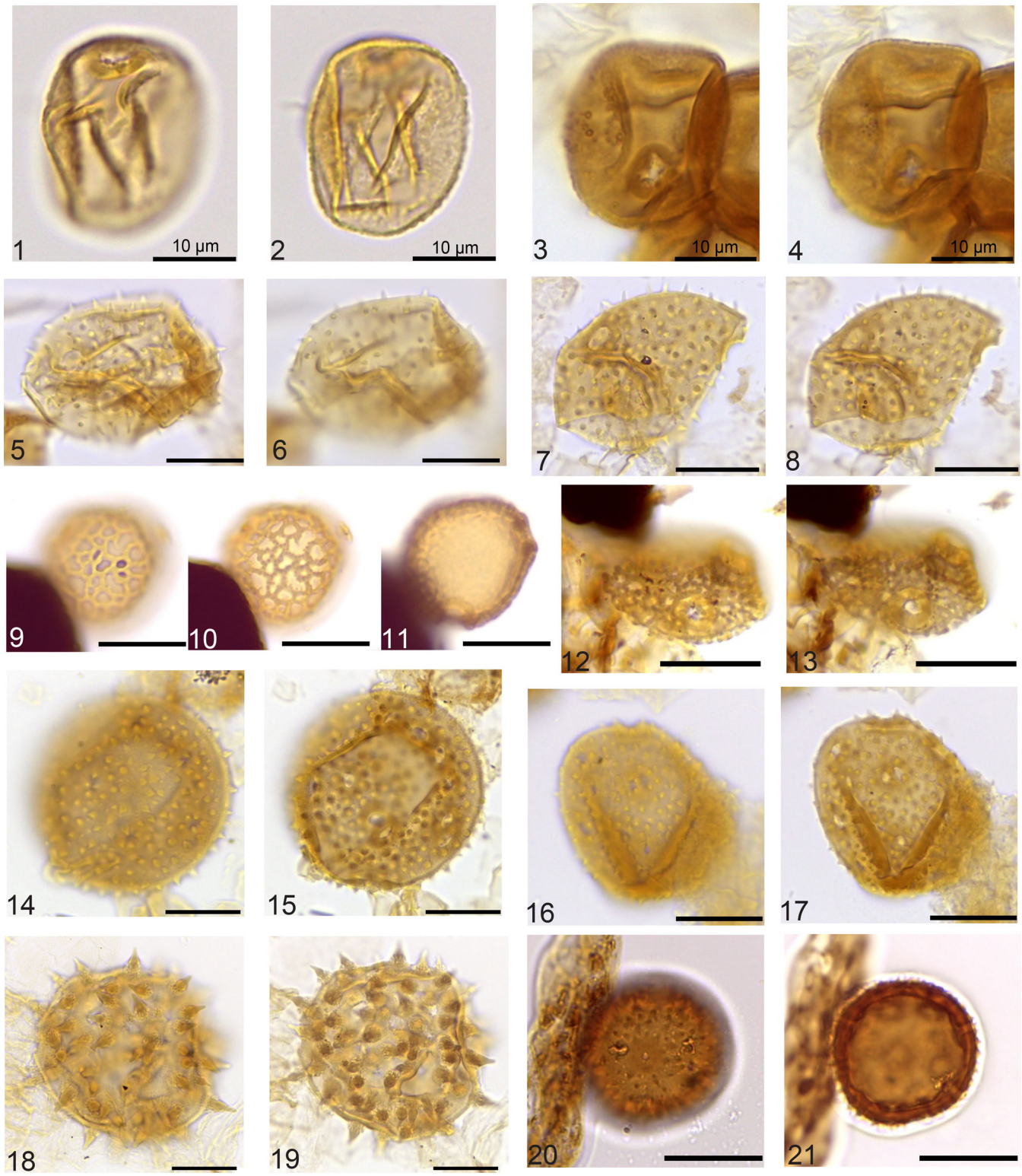

Plate 2. Figures 1, 2. *Monoporopollenites scabratus* sp. nov, holotype, 1AS-33-AM, 203.15 m (2), EF:C30. Figures 3, 4. *Monoporopollenites scabratus* sp. nov, paratype, 1AS-33-AM, 203.15 m (2), EF: Q44/4. Figures 5, 6. *Echitriporites jolyi* sp. nov., holotype, 1AS-33-AM, 232.18 m (1), EF: P55/3. Figures 7, 8. *Echitriporites jolyi* sp. nov., paratype, 1AS-33-AM, 232.18 m (1), EF: H41/3-J. Figures 9, 10, 11. *Retitriporites crassoreticulatus* sp. nov., holotype, 1AS-33-AM, 239.90 m (2), EF: W47/3. Figures 12, 13. *Retitriporites crassoreticulatus* sp. nov., paratype, 1AS-33-AM, 239.90 m (2), EF: X33/1. Figures 14, 15. *Echiperiporites germeraadii* sp. nov., holotype, 1AS-33-AM, 77.10 m (4), EF: N27/1. Figures 16, 17. *Echiperiporites germeraadii* sp. nov., paratype, 1AS-33-AM, 193.50 m (5), EF: J29. Figures 18, 19. *Echiperiporites estelae* Germeraad et al. 1968, 1AS-33-AM, 154.70 m (1), EF: L55/3. Figures 20, 21. *Echiperiporites jutaiensis* Silva-Caminha et al. 2010, holotype, 1AS-27-AM, 27-24, EF: E57 2. Scale bars: 20 µm, unless otherwise noted.

Original description. 'Monad, radial, isopolar, circular; pantoporate, endopores simple, 30 pores, pores 3 μm wide, 3 μm long, circular, evenly distributed over the entire grain, resembling a lophate ornamentation; tectate, exine 2.7 μm thick, nexine very thick, 2 μm thick, columellae 0.5 μm thick, distinct, 0.5 μm wide, 0.5 μm apart, columellae increase at the base of spines to 5 μm thick, tectum 0.2 μm thick; scupture echinate, echinae very long, 8–10 μm long, 3 μm wide, 5 μm apart, conical, echinae are restricted to the tectum surrounding the pores'.

New description. Monad, spheroidal; pantoporate, 30–50 pores, endopore simple, pores 2–3 μm wide, circular, evenly distributed over the entire grain; tectate, nexine 1 μm, columellae 4 μm tall, ≤0.5 μm wide; tectum 0.5 μm, smooth, tips of columellae distinct; sculpture echinate-lophate; ridges between echinae forming lophae; echinae conical, tips acute; echinae 5 μm tall, 4 μm wide at base, evenly distributed, 2–5 μm apart; lacunae of the lophae 5–7 wide, circular, 6–7 echinae per lophae.

Dimensions. Diameter 35–(43.6)–55 μm long × 30–(38.2)–42 μm wide (holotype = 48 × 42 μm, paratype = 55 × 41 μm); nm = 5, no = 100.

Remarks. In the holotype most of the lophae had lost the ridges between the echinae, except in a few places (Plate 3, figures 10–11). Some degraded grains lose all ridges and the echinae appear isolated (Plate 3, figures 12–13). We analyzed the holotype and established a paratype, increasing the pore number encompassed in this taxon (from 30 to 50).

Stratigraphic range. T15–T16.

Echiperiporites jaramilloi sp. nov.
Plate 3, figures 6–8

Holotype. 1AS-33-AM, 212.65 m (3), EF: P40/1-2.

Paratype. 1AS-33-AM, 238.33 m (3), EF: M38-M39.

Etymology. After the Colombian palynologist Carlos Jaramillo.

Diagnosis. Monad, spheroidal, large-sized, periporate, 23–25 pores, annulate, tectate, echinate, size of echinae 15–20 μm.

Description. Monad, spheroidal; periporate; 23–25 pores; tectate, nexine 3 μm, columellae 0.5–1 μm tall between spines and 2–3 μm underneath spines, ≤ 0.5 μm wide; tectum 0.5 μm, smooth, tips of columellae distinct; sculpture echinate; echinae conical, tips acute; echinae 15–20 μm tall, 8 μm wide at base, evenly distributed 10 μm apart; pores 5–7 μm wide, circular, annulate, annuli 2–4 μm wide, 5–6 μm thick.

Dimensions. Diameter 85–(103)–122 μm long × 85–(96.6)–112 μm wide (holotype = 122 × 112 μm, paratype = 108 × 98 μm); nm = 5, no = 14.

Comparisons. All other *Echiperiporites* species are smaller. *Echiperiporites estelae* is smaller and has echinae of 6–9 μm. *Echiperiporites titanicus* sp. nov. has more pores (>70).

Remarks. This species is similar to *Echiperiporites* spp. described in Hoorn (1994, p. 227, pl. 1, fig. 12).

Botanical affinity. *Hibiscus* (Malvaceae).

Stratigraphic range. T14–T16.

Echiperiporites titanicus sp. nov.
Plate 3, figures 9–12

Holotype. 1AS-33-AM, 399.10 m (1), EF: G46/2.

Paratype. 1AS-37-AM, 84.85 m (1), EF: T48/3-4.

Etymology. After the great thickness of the nexine.

Diagnosis. Monad, spheroidal, large sized, periporate, >70 pores, simple, tectate, echinate, size of echinae 12 μm.

Description. Monad, spheroidal; periporate; more than 70 pores; tectate, nexine 6 μm, columellae 1 μm tall; tectum <0.5 μm, smooth, tips of columellae distinct; sculpture echinate; echinae conical, tips acute; echinae 12 μm tall, 5–6 μm wide at base, evenly distributed 13 μm apart; pores circular, simple, 2 μm wide at ectopore and canal pore widens to 6 μm, pores 15 μm apart.

Dimensions. Diameter 78–(84)–90 μm long × 90 μm wide (holotype = 90 × 90 μm, paratype = 78 μm wide (incomplete)); nm = 2, no = 2.

Comparisons. *Echiperiporites estelae* has thinner exine and smaller spines (6–9μm). *Echiperiporites lophatus* Silva-Caminha et al. (2010) has lophae and is smaller. *Echiperiporites akanthos* Van der Hammen & Wymstra 1964 is much smaller in size, with smaller echinae. *Echiperiporites jaramilloi* sp. nov. is larger and has fewer pores (23–25).

Botanical affinity. *Malachra* (Malvaceae).

Stratigraphic range. T14.

PSILAPERIPORITES Regali et al. 1974

Type species. *Psilaperiporites robustus* Regali et al. 1974.

Psilaperiporites delicatus sp. nov.
Plate 3, figures 13–16

Holotype. 1AS-37-AM, 94.70 m (1), EF: G 30/4.

Paratype. 1AS-33-AM, 212.65 m (3), EF: T25/2.

Etymology. After the delicate appearance of the thin exine.

Diagnosis. Monad, spheroidal, large-sized, periporate, 6 pores, simple, atectate, psilate.

Description. Monad, amb spheroidal; periporate; 6 pores; atectate, exine 1–1.2 μm; sculpture psilate; pore 6–9 μm wide, simple, circular.

Dimensions. Diameter 24–(27.4)–32 μm long × 22–(25.2)–30 μm wide (holotype = 25 × 23 μm, paratype = 28 × 26 μm); nm = 5, no = 71.

Comparisons. *Psilaperiporites minimus* Regali et al. 1974 is tectate and has more pores (40–50). *Psilaperiporites robustus* Regali et al. 1974 is larger (45–63 μm). *Psilaperiporites suarezi* Vajda-Santibanez 1999 has more pores (16–34). *Parsonsidites*? sp. 1 Jaramillo & Dilcher (2001) is psilate-micropitted and pores have an annulus.

Stratigraphic range. T15–T16.

Psilaperiporites lunaris sp. nov.
Plate 3, figures 17–18

Holotype. 1AS-37-AM, 114 m (1), EF: K34.

Etymology. After its resemblance to the craters of the moon.

Diagnosis. Monad, spheroidal, small-sized, pantoporate, 6 pores, annulate, atectate, psilate.

Description. Monad, spheroidal; pantoporate; 6 pores; atectate, exine 1 μm, smooth; sculpture psilate; pores circular, annulate, 1 μm wide, annuli 1.5 μm thick, 1 μm wide, pores 5 μm apart.

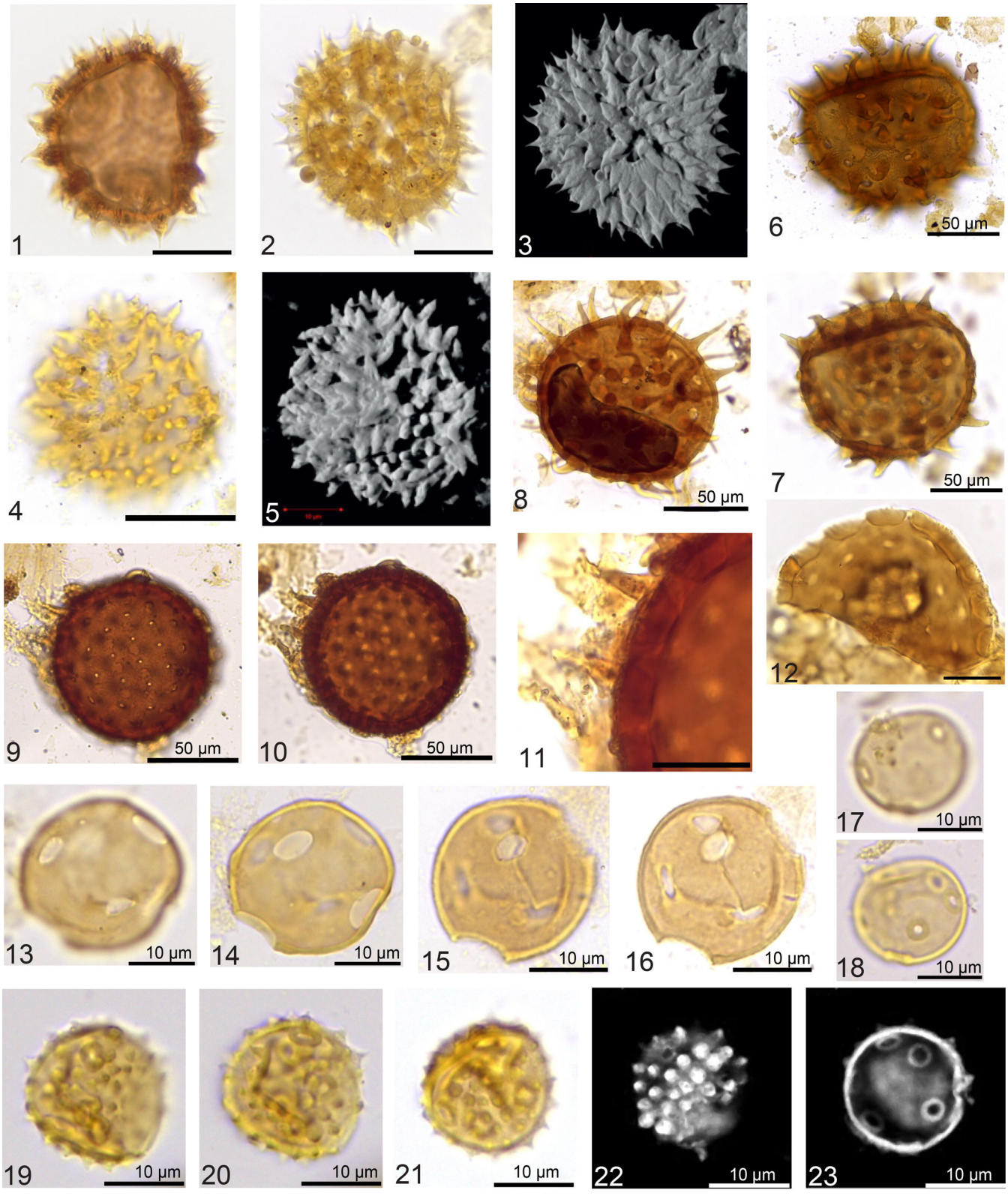

Plate 3. Figure 1. *Echiperiporites lophatus* (Silva Caminha, Jaramillo, & Absy 2010) emend., holotype, 1AS-27-AM, 27-7, EF: S24. Figures 2, 3. *Echiperiporites lophatus* (Silva Caminha, Jaramillo, & Absy 2010) emend., paratype, 1AS-33-AM, 154.70 m (3), EF: M54/1. Figures 4, 5. *Echiperiporites lophatus* (Silva-Caminha, Jaramillo and Absy 2010) emend., 1AS-33-AM, 137 m (1), EF T58/4. Figures 6, 7. *Echiperiporites jaramilloi* sp. nov., holotype, 1AS-33-AM, 212.65 m (3), EF: P40/1-2. Figure 8. *Echiperiporites jaramilloi* sp. nov., paratype, 1AS-33-AM, 238.33 m (3), EF: M38-M39. Figures 9, 10, 11. *Echiperiporites titanicus* sp. nov., holotype, 1AS-33-AM, 399.10 m (1), EF: G46/2. Figure 12. *Echiperiporites titanicus* sp. nov., paratype, 1AS-37-AM, 84.85 m (1), EF: T48/3-4. Figures 13, 14. *Psilaperiporites delicatus* sp. nov., holotype, 1AS-37-AM, 94.70 m (1), EF: G 30/4. Figures 15, 16. *Psilaperiporites delicatus* sp. nov., paratype, 1AS-33-AM, 212.65 m (3), EF: T25/2. Figures 17, 18. *Psilaperiporites lunaris* sp. nov., holotype, 1AS-37-AM, 114 m (1), EF: K34. Figures 19, 20. *Echistephanoporites annulatus* sp. nov., holotype, 1AS-37-AM, 114 m (1), EF: G41/4. Figures 21, 22, 23. *Echistephanoporites annulatus* sp. nov., paratype, 1AS-37-AM, 114 m (1), EF: U33. Scale bars: 20 µm, unless otherwise noted.

Dimensions. Diameter 17 μm long × 18 μm wide (holotype); nm = 1, no = 1.
Comparisons. *Psilaperiporites* sp. 1 Silva-Caminha et al. (2010) has 18 pores arranged in pairs. *Psilaperiporites minimus* Regali et al. 1974 is tectate, with more pores (40–50). *Psilaperiporites robustus* Regali et al. 1974 is larger (45–63 μm). *Multiporopollenites pauciporatus* Jaramillo & Dilcher (2001) is tectate and micro-foveolate.
Stratigraphic range. T16.

STEPHANOPORATE

ECHISTEPHANOPORITES Leidelmeyer 1966

Type species. *Echistephanoporites alfonsi* Leidelmeyer 1966.

Echistephanoporites annulatus sp. nov.
Plate 3, figures 19–23

Holotype. 1AS-37-AM, 114 m (1), EF: G41/4.
Paratype. 1AS-37-AM, 114 m (1), EF: U33.
Etymology. After the annulate pores.
Diagnosis. Monad, spheroidal, small-sized, stephanoporate, 5–6 pores, annulate, tectate, echinate, echinae 1 μm.
Description. Monad, spheroidal; stephanoporate; 5–6 pores; tectate, columellae indistinct, exine 1 μm, smooth; sculpture echinate; echinae conical, tips acute; echinae 1.5 μm tall, 2 μm wide at base, closely distributed; pores circular, annulate, 1 μm wide, annuli 1 wide, pores 4 μm apart.
Dimensions. Diameter 17–(17.8)–19 μm long × 17–(17.8)–19 μm wide (holotype = 18 × 18 μm, paratype = 17 × 17 μm); nm = 5, no = 8.
Comparisons. *Echistephanoporites alfonsi* Leidelmeyer 1966 is tectate, has 4 pores and has echinae 1 μm thick. *Echiperiporites akanthos* Van der Hammen & Wymstra 1964 is pantoporate and has echinae of a different size.
Stratigraphic range. T16.

TRICOLPATE

ECHITRICOLPITES Regali, Uesugui & Santos 1974

Type species. *Echitricolpites communis* Regali, Uesugui & Santos 1974.

Echitricolpites cruziae sp. nov.
Plate 4, figures 1–4

Holotype. 1AS-33-AM, 155 m (6), EF: F49/4.
Paratype. 1AS-33-AM, 155 m (6), EF: J52/3-K.
Etymology. After the Brazilian palynologist Norma Cruz.
Diagnosis. Monad, spheroidal, mid-sized, tricolpate, intectate, echinate, echinae <1 μm.
Description. Monad; spheroidal; echinate; tricolpate; intectate, nexine 1.2 μm; sculpture echinate; echinae 0.51 μm; colpi 8–11 μm long, 2 μm wide, simple; occasionally the grain seems to be inaperturate.
Dimensions. Polar view diameter 30–(30.5)–31.5 μm long × 27–(29.2)–30 μm wide (holotype = 31.5 × 30 μm, paratype = 30 × 39 μm); nm = 5, no = 61.
Comparisons. *Echitricolpites communis* Regali et al. 1974 has thin echinae and distinct columellae. *Echitricolpites polaris* Regali et al. 1974 is larger (45–50 μm), colporate and prolate. *Malvacipolloides romeroe* sp. nov. is tectate and tricolporate.
Stratigraphic range. T16.
Botanical affinity. *Aegiphila* (Lamiaceae).

LADAKHIPOLLENITES Mathur & Jain 1980

Type species. *Ladakhipollenites levis* (Sah & Dutta 1966) Mathur & Jain

1980 *Ladakhipollenites carmoi* sp. nov.
Plate 4, figures 5–8

Holotype. 1AS-37-AM, 84.85 m (1), EF: J27/2.
Paratype. 1AS-37-AM, 84.85 m (1), EF: H26/2.
Etymology. After the Brazilian ostracodologist Dermeval A. do Carmo.
Diagnosis. Monad, prolate, large-sized, tricolpate, tectate, psilate-foveolate.
Description. Monad, prolate; tricolpate; tectate, exine 2 μm, nexine 0.5 μm, columellae 0.5 μm tall, 0.3 μm wide, 0.5 μm apart, tectum 1 μm; sculpture psilate to slightly foveolate; colpi simple, invaginating, 50 μm long.
Dimensions. Polar diameter 54–(56.2)–60 μm, equatorial diameter 26–(28.6)–31 μm (holotype = 55 × 26 μm, paratype = 55 × 26 μm); nm = 5, no = 16.
Comparisons. *Ladakhipollenites*? *caribbiensis* (Muller et al. 1987) Silva Caminha et al. 2010 is tricolporate. *Ladakhipollenites simplex* (Gonzalez 1967) Jaramillo & Dilcher (2001) has marginate colpi and thinner tectum. *Psilatricolpites clarissimus* (van der Hammen 1954) van der Hammen & Wymstra 1964 is smaller in equatorial length (30 μm) and psilate.
Stratigraphic range. T16.

RETIBREVITRICOLPITES Van Hoeken-Klinkenberg 1966

Type species. *Retibrevitricolpites triangulatus* van Hoeken-Klinkenberg 1966.

Retibrevitricolpites microreticulatus sp. nov.
Plate 4, figures 9–12

Holotype. 1AS-33-AM, 276 (3), EF: P37-Q.
Paratype. 1AS-33-AM, 190 (4), EF: G44.
Etymology. After the microreticulate ornamentation.
Diagnosis. Monad, spheroidal, mid-sized, tricolpate, semitectate, microreticulate.
Description. Monad; spheroidal; tricolpate; semitectate, exine 3 μm, nexine 1.2 μm, columellae clava-like, 0.8 μm high, capita merged forming tectum, tectum 1 μm; sculpture microreticulate, lumina 0.8 μm, muri 0.5 μm; colpi simple, pointed tips, 12 μm long.
Dimensions. Equatorial view diameter 22–(26)–27 μm, polar diameter 20–(26)–30 μm (holotype = 30 × 27 μm); polar view diameter 29 μm long, 28 μm wide (paratype); nm = 5, no = 11.

Comparisons. *Clavainaperturites microclavatus* Hoorn 1994 is inaperturate and micropitted. *Retitricolporites crucipori* Muller 1968 has wider lumina (>2 μm). *Retitricolporites constrictus* Gonzalez 1967 has colpi costate. *Retitricolporites gemmatus* Herngreen 1975 has exine thinning toward colpi. *Tricolpites microreticulatus* Belsky et al. 1965 has a triangular-obtuse-convex shape and longer colpi.
Stratigraphic range. T16.

ROUSEA Srivastava 1969

Type species. *Rousea subtilis* Srivastava 1969.

Rousea cavitata sp. nov.
Plate 4, figures 13–14

Holotype. 1AS-33-AM, 232 (1), EF: R37/3.
Etymology. After the internal cavities of the muri.
Diagnosis. Monad, subtriangular, mid-sized, tricolpate, semitectate, reticulate, heterobrochate.
Description. Monad, amb subtriangular; tricolpate; semitectate, exine 6 μm, nexine 1.5 μm, simplicolumellate, columellae hollow, 1.5 μm tall, outline round to elongate, 1–3 μm wide, tectum 3 μm; sculpture reticulate, heterobrochate, lumina 2–7 μm, decreasing toward apocolpia, muri 2–3 μm, muri with internal cavities; colpi simple, rounded tips, 40 μm long.
Dimensions. Polar view diameter 55 μm long, 54 μm wide (holotype); nm = 1, no = 1.
Comparisons. *Rousea geranioides* (Couper 1960) Srivastava 1975 and *R. delicipollis* Srivastava 1975 are thinner and have smaller lumina and muri. *Rousea georgensis* (Brenner) Dettmann 1973 is smaller.
Stratigraphic range. T16.

STEPHANOCOLPATE

RETISTEPHANOCOLPITES Leidelmeyer 1966

Type species. *Retistephanocolpites angeli* Leidelmeyer 1966.

Retistephanocolpites curvimuratus sp. nov.
Plate 4, figures 15–18

Holotype. 1AS-33-AM, 326.25 m (1), EF: X34.
Paratype. 1AS-33-AM, 399.10 m (1), EF: S38/2.
Etymology. After the curvimurate pattern of ornamentation.
Diagnosis. Monad, circular, mid-sized, stephanocolpate, semitectate, reticulate, homobrochate.
Description. Monad; amb circular; stephanocolpate; semitectate, exine 4 μm, tectum 1 μm, columellae 2 μm, nexine 1 μm, sculpture reticulate; curvimurate, homobrochate, lumina irregular, varying from 1 to 4 μm; 5-colpate, colpi 10 μm long, 5 μm wide, costate, costae 2 μm thick, 2 μm wide. Sometimes in polar view grains seem colporate.
Dimensions. Polar view diameter 34–(39)–42 μm long × 32–(36.5)–38 μm wide (holotype = 42 × 38 μm, paratype = 42 × 38 μm); nm = 4, no = 5.
Intraspecific variability. Grains that were 4-colpate were observed.
Comparisons. *Retistephanocolpites angeli* Leidelmeyer 1966 has shorter colpi and lumina. *Retistephanocolpites regularis* van Hoeken-Klinkenberg 1966 is smaller (24.5 μm) and has smaller lumina. *Retistephanocolpites gracilis* Regali et al. 1974 is smaller and has more colpi (6–9). *Retistephanocolpites quadraticus* D'Apolito et al. 2019 has lumina 0.5 μm wide and simple colpi.
Stratigraphic range. T15–T16.

Retistephanocolpites pardoi sp. nov.
Plate 4, figures 19–20

Holotype. 1AS-37-AM, 96.65 m (2), EF: S35/2.
Etymology. After the Colombian palynologist Andres Pardo.
Diagnosis. Monad, circular, mid-sized, stephanocolpate, tectate, reticulate, homobrochate.
Description. Monad; amb circular; stephanocolpate; tectate, exine 2 μm; nexine 0.8 μm, columellae 1 μm visible under tectum, tectum 0.2 μm; sculpture reticulate supratectate, lumina irregular, 2–5 μm, muri 0.7 μm; colpi simple, 5 colpi, pointed tips, 20 μm long.
Dimensions. Polar view diameter 40 μm long × 39 μm wide (holotype); nm = 1, no = 1.
Comparisons. *Retistephanocolpites regularis* van Hoeken-Klinkenberg 1966 is smaller (24.5 μm) and lumina smaller. *Stephanocolpites costatus* Van der Hammen 1954 is smaller (26 μm) with smaller lumina. *Retistephanocolpites fossulatus* Jaramillo & Dilcher (2001) is also foveolate. *Retistephanocolpites circularis* Silva-Caminha et al. (2010) has shorter and marginate colpi.
Botanical affinity. *Amphilophium*? (Bignoniaceae).
Stratigraphic range. T16.

TRICOLPORATE

CICHOREACIDITES Sah 1967

Type species. *Cichoreacidites spinosus* Sah 1967.

Cichoreacidites? *flammulatus* sp. nov.
Plate 5, figures 1–6

Holotype. 1AS-33-AM, 262 m (2), EF: D46/2.
Paratype. 1AS-33-AM, 149.40 m (5), EF: K34-L34.
Etymology. After the resemblance of the conical thickenings in the tectum to the shape of a flame.
Diagnosis. Monad, spheroidal, mid-sized, lophate, curvimurate, periporate?
Description. Monad, spheroidal; lophate; apparently periporate; tectate, exine 2 μm tall, stratified in infratectum, 2 μm tall, and tectum 1 μm tall with thickenings separated by perforations. Confocal images show infratectum with uniserial cylindrical thickenings and tectum with conical thickenings that in optical microscope look like columellae and spines, respectively; nexine indistinct; lophae curvimurate, 3–5 μm wide, muri 1.5 μm wide.
Dimensions. Diameter 33–(36.6)–40 μm long, 31–(34)–36 μm wide (holotype = 33 × 33 μm, paratype = 40 × 35 μm); nm = 5, no = 20.

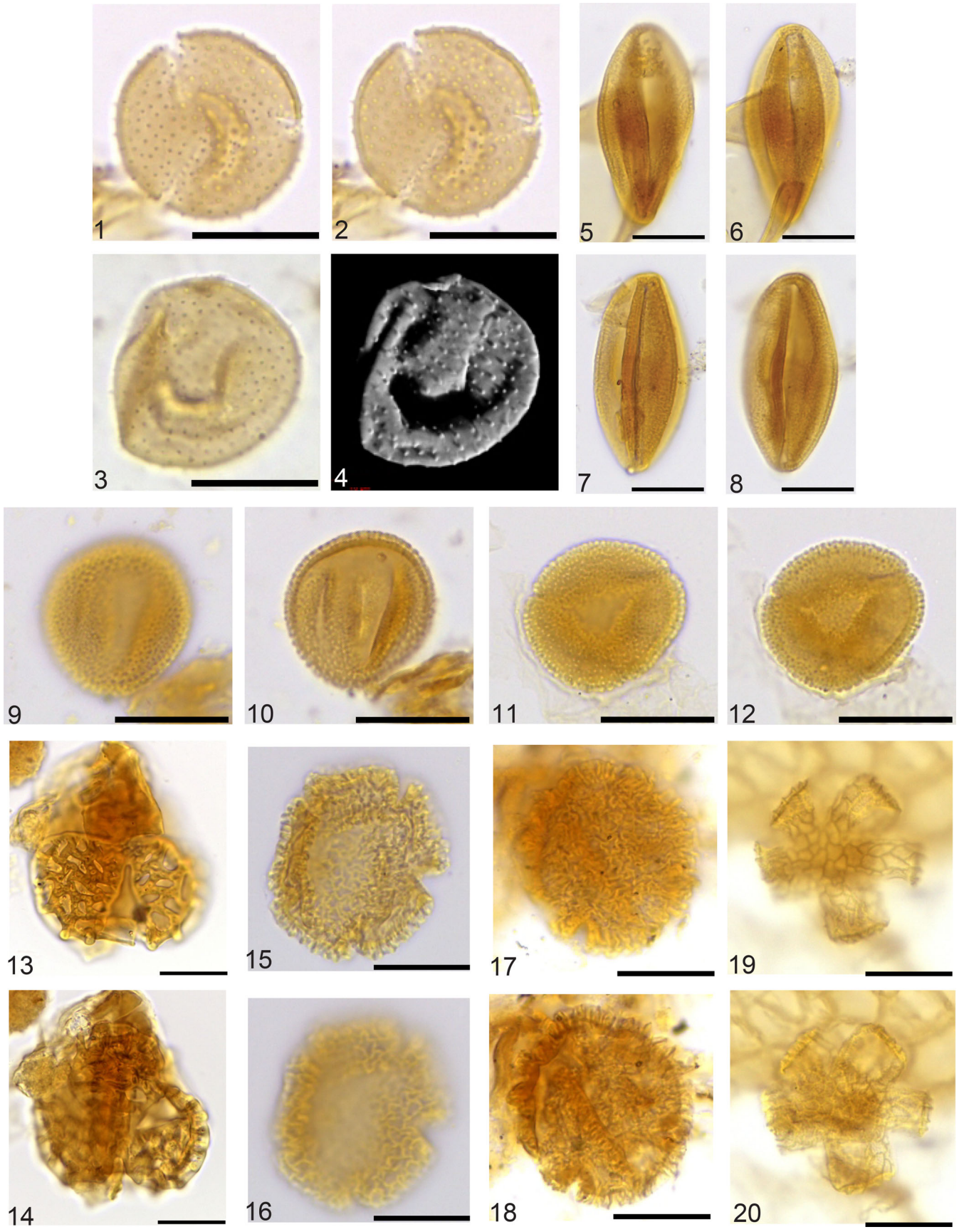

Plate 4. Figures 1, 2. *Echitricolpites cruziae* sp. nov., holotype, 1AS-37-AM, 155 m (6), EF: F49/4. Figures 3, 4. *Echitricolpites cruziae* sp. nov., paratype, 1AS-37-AM, 155 m (6), EF: J52/3-K. Figures 5, 6. *Ladakhipollenites carmoi* sp. nov., holotype, 1AS-37-AM, 84.85 m (1), EF: J27/2. Figures 7, 8. *Ladakhipollenites carmoi* sp. nov., paratype, 1AS-37-AM, 84.85 m (1), EF: H26/2. Figures 9, 10. *Retibrevitricolpites*? *microreticulatus* sp. nov., holotype, 1AS-33-AM, 276 (3), EF: P37-Q. Figures 11, 12. *Retibrevitricolpites*? *microreticulatus* sp. nov., paratype, 1AS-33-AM, 190 (4), EF: G44. Figures 13, 14. *Rousea cavitata* sp. nov., holotype, 1AS-33-AM, 232 (1), EF: R37/3. Figures 15, 16. *Retistephanocolpites curvimuratus* sp. nov., holotype, 1AS-33-AM, 326.25 m (1), EF: X34. Figures 17, 18. *Retistephanocolpites curvimuratus* sp. nov., paratype, 1AS-33-AM, 399.10 m (1), EF: S38/2, Figures 19, 20. *Retistephanocolpites pardoi* sp. nov., holotype, 1AS-37-AM, 96.65 m (2), EF: S35/2. Scale bars: 20 μm.

Comparisons. *Cichoreacidites longispinosus* (Lorente 1986) Silva-Caminha et al. (2010) is tricolporate and echinate. *Cichoreacidites*? *igapoensis* D'Apolito et al. 2019 has higher columella and muri is psilate. *Fenestrites gemmatus* Regali et al. 1974 is gemmate.
Remarks. *Cichoreacidites* Sah 1967 accommodates lophate grains, with spines on the ridges. There is no published genus that encompasses the specific characteristics of *Cichoreacidites*? *flammulatus* sp nov., so it is placed provisionally in this genus.
Stratigraphic range. T16.

FOVEOTRICOLPORITES Pierce 1961

Type species. *Foveotricolporites rhombohedralis* Pierce 1961.

Foveotricolporites crassus sp. nov.
Plate 5, figures 7–9

Holotype. 1AS-33-AM, 276.70 m (3), EF: G44.
Paratype. 1AS-33-AM, 282.55 m (1), EF: H35.
Etymology. After the thickness of the exine.
Diagnosis. Monad, subtriangular, large-sized, tricolporate, pore indistinct, intectate, foveolate.
Description. Monad, amb subtriangular; tricolporate; intectate, exine 3 μm, stratification indistinct; sculpture foveolate, foveolae <1 μm, 1–2 μm apart; colpi costate, pointed tips, 22 μm long, costae 3 μm wide, pore indistinct.
Dimensions. Polar view diameter 24–(58.5)–60 μm long, 52–(56)–60 μm wide (holotype = 63 × 60 μm, paratype = 54 × 52 μm); nm = 2, no = 2.
Comparisons. *Foveotricolporites crassiexinatus* van Hoeken-Klinkenberg 1966 is smaller (31 μm) with costate endopores. *Foveotricolporites fossulatus* Jaramillo & Dilcher (2001) is also fossulate. *Lanagiopollis crassa* (Van der Hammen & Wymstra 1964) Frederiksen 1988 has longer colpi and is smaller, with distinct columellae and variable ornamentation from psilate to reticulate.
Stratigraphic range. T15–T16.

GOMPHRENIPOLLIS Anzótegui & Cuadrado 1996

Type species. *Gomphrenipollis pintadensis* Anzótegui & Cuadrado 1996.

Gomphrenipollis garciae sp. nov.
Plate 5, figures 10–14

Holotype. 1AS-33-AM, 276.70 m (2), EF: Q39.
Paratype. 1AS-33-AM, 399.10 m (1), EF: T45.
Etymology. After the Brazilian palynologist Maria Judite Garcia.
Diagnosis. Monad, spheroidal, mid-sized, lophate, curvimurate, periporate?, semitectate.
Description. Monad, spheroidal; apparently periporate; semitectate, exine 3.5 μm tall, columellae digitate, 2 μm tall, tectum 1.5 μm tall, muri slightly pointed at the corners of the lophae, nexine indistinct; lophate, polygonal to slightly curvimurate, lumina 4–8 μm wide, muri 1.5 μm wide.
Dimensions. Diameter 28–(29.8)–33 μm long, 27–(29.2)–32 μm wide (holotype = 30 × 29 μm, paratype = 28 × 27 μm); nm = 5, no = 11.
Comparisons. *Gomphrenipollis minimus* Silva-Caminha et al. (2010) is smaller, without digitate columellae. *Fenestrites spinosus* Van der Hammen 1956 and *Cichoreacidites longispinosus* (Lorente 1986) Silva-Caminha et al. (2010) are echinate. *Cichoreacidites*? *igapoensis* D'Apolito et al. (2019) is larger and not curvimurate.
Botanical affinity. Amaranthaceae?
Stratigraphic range. T14–T16.

MALVACIPOLLOIDES Anzotégui & Garalla 1986

Type species. *Malvacipolloides densiechinata* Anzotégui & Garalla 1986.

Malvacipolloides diversus sp. nov.
Plate 5, figures 15–19

Holotype. 1AS-37-AM, 114 m (2), EF: S48/1.
Paratype. 1AS-33-AM, 148.58 m (4), EF: N44.
Etymology. After the variability of the echinae.
Diagnosis. Monad, spheroidal, mid-sized, tricolporate, colpi simple, pore annulate, echinate, tectate.
Description. Monad; spheroidal; tricolporate; tectate, nexine 1.2 μm, columella 0.6 μm tall, clava-shaped; tectum 0.4 μm; sculpture echinate; echinae vary in size and shape, tips rounded or acute; echinae 6–7 μm tall, 2–4 μm wide at base, tectum thicker underneath forming a disk at the base of the echinae 2 μm thick, 7 μm wide, sparsely distributed, 5 μm apart; interspine surface micropitted; ectocolpi short, simple, 9–10 μm long; endopore 4 μm wide, circular, annulate, annuli 4 μm wide.
Dimensions. Diameter 47–47 μm long, 30–(38.5)–47 μm wide (holotype = 47 × 47 μm, paratype 47 × 30 μm, folded); nm = 2, no = 2.
Comparisons. *Malvacipolloides maristellae* (Muller et al. 1987) Silva-Caminha et al. (2010) is brevicolpate, with thin and smooth tectum and smaller echinae (2–4 μm) (Espinosa et al. 2020). *Malvacipolloides comodoroensis* Barreda 1993 has shorter colpi and shorter echinae. *Malvacipolloides densiechinata* Anzotégui & Garalla 1986 has a shorter interspine distance and its echinae have swollen bases.
Stratigraphic range. T16.

Malvacipolloides echibaculatus sp. nov.
Plate 6, figures 1–5
Malvacipolloides sp. 2 Silva-Caminha et al. 2010, p. 62, Plate 6, figures 6–7.

Holotype. 1AS-37-AM, 96.35 m (1), EF: T34/1-2.
Paratype. 1AS-37-AM, 34.90 m (2), EF: B33/C34.
Etymology. After the variability of the tips of the echinae.
Diagnosis. Monad, spheroidal, mid-sized, tricolporate, echinate, with some tips of spines varying in shape, tectate.
Description. Monad; spheroidal; tricolporate; tectate, exine 1.5 μm, nexine 0.6 μm, columellae 0.6 μm, tectum 0.3 μm; sculpture echinate, echinae 3–5 μm tall, base 0.2–0.3 μm wide, conical. The tip of spines varies between acute and blunt, occasionally forked. Sparsely and unevenly distributed. Distance between spines varies between 0.7 and 1.5 μm. Microreticulate

ornamentation interspines, lumina rounded, <0.5 μm. Colpi short, 10–12 μm long, simple; pores indistinct.

Dimensions. Polar view diameter 32–(37)–42 μm long, 32–(36.4)–39 μm (holotype = 42 × 39 μm, paratype = 39 × 38 μm); nm = 5, no = 28.

Comparisons. *Malvacipolloides maristellae* (Muller et al. 1987) Silva-Caminha et al. (2010) has different wall structure, with columella height increasing underneath spines. *Brevitricolpites microechinatus* Jaramillo & Dilcher (2001) is intectate. *Brevitricolpites* sp. 1 Jaramillo & Dilcher (2001) has smaller spines (<1 μm). *Brevitricolpites variabilis* Gonzalez 1967 is clavate to gemmate. *Malvacipolloides diversus* sp. nov. has annulate pores.

Stratigraphic range. T16.

Malvacipolloides romeroae sp. nov.
Plate 6, figures 6–10
Malvacipolloides? sp. 3 Silva-Caminha et al. 2010, p. 62, Plate 6, figures 8–9.

Holotype. 1AS-27-AM, AM27-22, EF: Y70/1.

Paratype. 1AS-33-AM, 239.90 m (2), EF: D34.

Etymology. After the Colombian palynologist Millerlandy Romero Baez.

Diagnosis. Monad, spheroidal, mid-sized, tricolp(or)ate, colpi costate, echinate, tectate.

Description. Monad; spheroidal; tricolp(or)ate; tectate, nexine 0.3 μm, columella 0.5 μm, tectum 0.2 μm; sculpture echinate; echinae 0.5 μm tall, sparsely distributed 2–3 μm apart; colpi costate, 14 μm long, costae 3 μm wide, tapering toward colpi ends; ends pointed; pore simple, circular, 5 μm wide; apocolpium 15 μm wide. Both colpate and colporate grains have been seen.

Dimensions. Polar view diameter 26–(30.2)–34 μm long, 26–(29.6)–33 μm wide (holotype = 33 × 31 μm, paratype = 34 × 33 μm); nm = 5, no = 8.

Comparisons. *Brevitricolpites microechinatus* Jaramillo & Dilcher (2001) is intectate and its pore is costate. *Echitricolporites mcneillyi* Germeraad et al. (1968) is smaller (23 μm).

Stratigraphic range. T16.

MARGOCOLPORITES (Ramanujam 1966 ex Srivastava 1969) Pocknall & Mildenhall 1984

Type species. *Margocolporites tsukadai* (Ramanajuan 1966) Srivastava 1969.

Margocolporites carinae sp. nov.
Plate 6, figures 11–14

Holotype. 1AS-33-AM, 77.10 m (6), EF: F48/2.

Paratype. 1AS-33-AM, 203.15 m (2), EF: H43-J.

Etymology. After the Dutch palynologyst Carina Hoorn.

Diagnosis. Monad, mid-sized, tricolporate, colpi costate, costa divided by a thinning of the exine, tectate, psilate.

Description. Monad, amb circular; tricolporate; tectate, exine 1 μm in mesocolpi, nexine 0.5 μm, tectum 0.5 μm; columellae indistinct, sculpture psilate, ectocolpi costate, costae divided by a thinning of the exine, external costae 2 μm wide, thinning 1.5 μm wide, costae 2 μm wide, 2.5 μm thick, colpi 6 μm long, 4 μm wide; rounded tips, pore simple, circular, 4 μm.

Dimensions. Polar view diameter 26–(33)–37 μm long, 26–(30.8)–35 μm wide (holotype = 37 × 32 μm, paratype = 33 × 31 μm); nm = 5, no = 35.

Comparisons. *Margocolporites rauvolfii* Salard-Cheboldaeff 1978 does not have external costae; the margo is formed by a thinning of the exine all around the colpi. *Margocolporites vanwijhei* Germeraad et al. (1968) and *M. mandjicus* Boltenhagen 1976 are reticulate. *Margocolporites fastigiatus* Silva-Caminha et al. (2010) is fastigiate and micropitted.

Botanical affinity. *Rauvolfia* (Apocynaceae).

Stratigraphic range. T15–T16.

MULTIAREOLITES Germeraad et al. 1968

Type species. *Multiareolites formosus* (Van Der Hammen 1956) Germeraad et al. 1968.

Multiareolites? *reticulatus* sp. nov.
Plate 6, figures 15–20

Holotype. 1AS-33-AM, 186.60 m (2), EF: Q41/4-R.

Paratype. 1AS-33-AM, 203 (2): EF: H33.

Etymology. After the reticulate ornamentation.

Diagnosis. Monad, large-sized, tricolporate, semitectate, reticulate, homobrobrochate, also areolate along colpi.

Description. Monad, prolate; tricolporate; semitectate, exine 3 μm, nexine 1.5 μm, columellae 0.7 μm tall, tectum 0.7 μm; sculpture reticulate, homobrochate, lumina rounded ±1 μm, muri ±1 μm; ectocolpi marginate, tips pointed, 34 μm long, <1 μm wide, margo formed by one row of areoli, areoli 5–6 μm wide, 1–2 μm apart, areoli from the extremities elongated toward the end of the colpi; endopore annulate, 3 μm wide, annuli 1 μm wide.

Dimensions. Polar diameter 42–(46)–50 μm, equatorial diameter 25–(28)–31 μm (holotype = 50 × 31 μm, paratype = 42 × 25 μm); nm = 2, no = 2.

Comparisons. *Multiareolites formosus* (Van der Hammen 1956) Germeraad et al. (1968) is dicolporate and not reticulate.

Remarks. The genus *Multiareolites* was created to accommodate the pollen of *Adhatoda*, *Anisotus*, *Beloperone*, *Dianthera*, *Jacobinia*, *Justicia*, *Kolobochilus*, *Monechma* and *Rungia* (Acanthaceae) (Germeraad et al. 1968), and it is described as dicolporate. However, the extant genera *Anisotes*, *Dicliptera* and *Hypoestes* (Acanthaceae) present similar morphology, but can be tricolporate (Al-Hakimi et al. 2017).

Botanical affinity. Acanthaceae.

Stratigraphic range. T16.

RANUNCULACIDITES Sah 1967

Type species. *Ranunculacidites communis* Sah 1967.

Ranunculacidites reticulatus sp. nov.
Plate 7, figures 1–3

Holotype. 1AS-37-AM, 96.65 m (2), EF: S35/2.

Etymology. After the reticulate ornamentation.

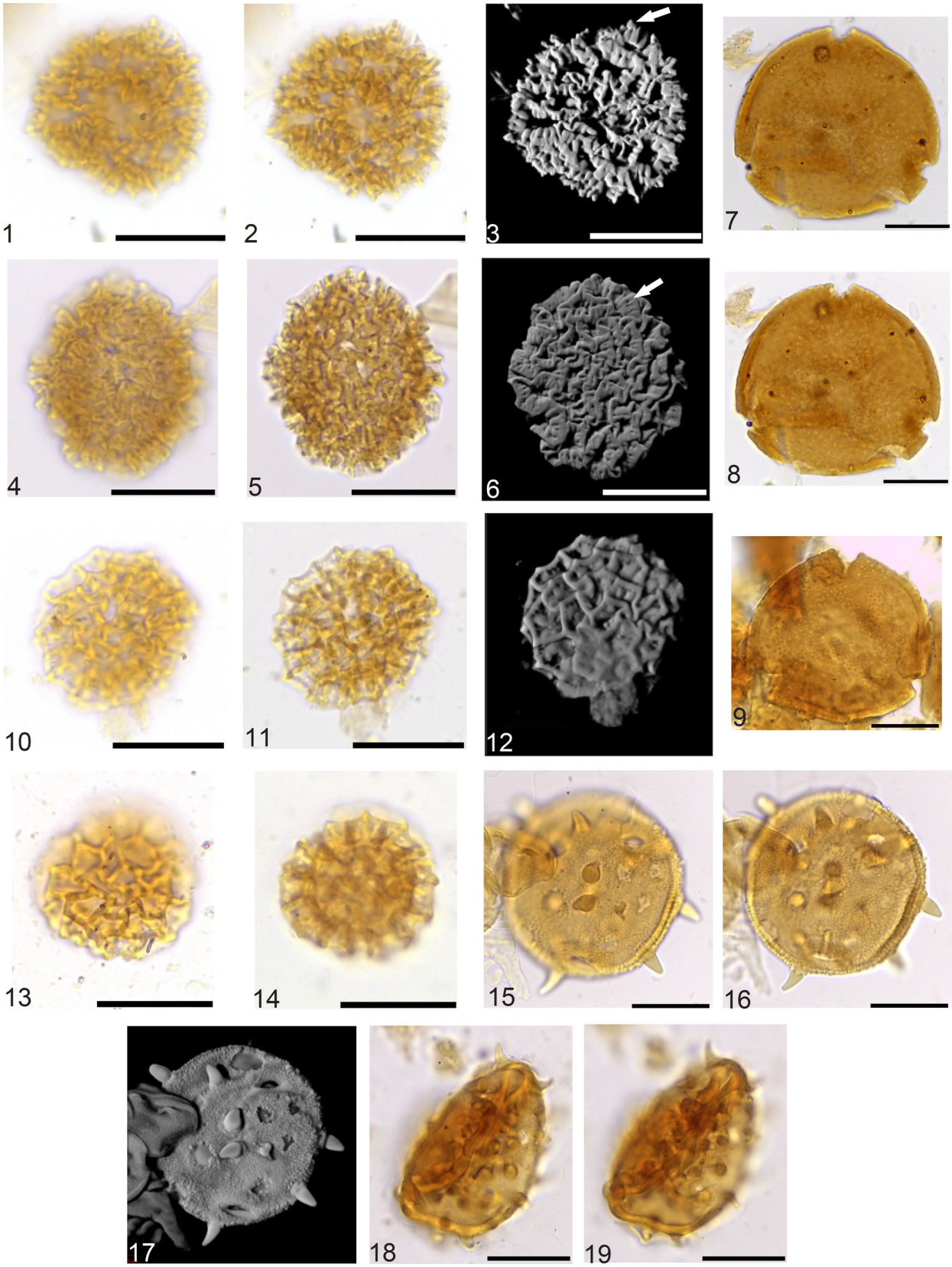

Plate 5. Figures 1, 2, 3. *Cichoreacidites*? *flammulatus* sp. nov., holotype, 1AS-33-AM, 262 m (2), EF: D46/2. Figure 3. White arrow: uniserial cylindrical thickenings and tectum with conical thickenings. Figures 4, 5, 6. *Cichoreacidites*? *flammulatus* sp. nov., paratype, 1AS-33-AM, 149.40 m (5), EF: K34-L34. Figure 6. White arrow: tectum thickenings separated by perforations. Figures 7, 8. *Foveotricolporites crassus* sp. nov., holotype, 1AS-33-AM, 276.70 m (3), EF: G44. Figures 9. *Foveotricolporites crassus* sp. nov. paratype, 1AS-33-AM, 282.55 m (1), EF: H35. Figures 10, 11, 12. *Gomphrenipollis garciae* sp. nov., holotype, 1AS-33-AM, 276.70 m (2), EF: Q39. Figures 13, 14. *Gomphrenipollis garciae* sp. nov., paratype, 1AS-33-AM, 399.10 m (1), EF: T45. Figures 15, 16, 17. *Malvacipolloides diversus* sp. nov., holotype, 1AS-37-AM, 114 m (2), EF: S48/1. Figures 18, 19. *Malvacipolloides diversus* sp. nov. paratype, 1AS-33-AM, 148.58.33 m (4), EF: N44. Scale bars: 20 μm.

Diagnosis. Monad, mid-sized, tricolporate, colpi operculate, semitectate, reticulate, heterobrochate, endopore indistinct.

Description. Monad, prolate; tricolporate; semitectate, exine 2.5 μm, nexine 1.5 μm, columellae clava-like, 0.5 μm tall, capita merged forming tectum, tectum 0.5 μm; sculpture reticulate, heterobrochate, lumina 0.5–1.5 μm smaller toward apocolpia, muri 1 μm; ectocolpi marginate, rounded tips, with operculum, 13 μm long, 5 μm wide; endopore indistinct.

Dimensions. Diameter 32 μm long, 31 μm wide (holotype); nm = 1, no = 1.

Comparisons. *Ranunculacidites operculatus* (Van der Hammen & Wymstra 1964) Jaramillo & Dilcher (2001) is tectate and has psilate-micropitted ornamentation. *Ranunculacidites communis* Sah 1967 is tricolpate, with longer colpi and finely reticulate.

Stratigraphic range. T16.

RETIBREVITRICOLPORITES Legoux 1978

Type species. *Retibrevitricolporites obodoensis* Legoux 1978.

Retibrevitricolporites costaporus sp. nov.
Plate 7, figures 4–7

Holotype. 1AS-33-AM, 158.20 m (1), EF: G54.

Paratype. 1AS-33-AM, 158.20 m (1), EF: H49.

Etymology. After the costae of the pore.

Diagnosis. Monad, mid-sized, tricolporate, brevicolpate, colpi simple, semitectate, simplicolumellate, homobrochate, lumina irregular, pores circular, costate.

Description. Monad, amb triangular-obtuse-convex; tricolporate; semitectate, exine 1.5 μm, nexine 0.5 μm, tectum 0.5 μm; columellae 0.5 μm, simplicolumellate, sculpture reticulate, homobrochate, lumina irregular varying from 2 to 3 μm, muri 1 μm; ectocolpi simple, pointed tips, 10 μm long, 1 μm wide; endopore costate, circular, costae 4 μm wide, 13 μm thick.

Dimensions. Polar view diameter 30–(34)–38 μm long, 30–(30.8)–32 μm wide (holotype = 37 × 32 μm, paratype = 31 × 29 μm); nm = 5, no = 55.

Comparisons. *Retibrevitricolporites*? *toigoae* sp. nov. is tectate with suprareticulum. *Foveotricolporites pseudodubiosus* Silva-Caminha et al. (2010) is foveolate and heterobrochate. *Retibrevitricolporites protrudens* Legoux 1978 has strongly protruding apertures. *Retibrevitricolporites grandis* Jaramillo & Dilcher (2001) has fine reticulum and indistinct pores. *Retibrevitricolporites speciosus* Jaramillo & Dilcher (2001) is strongly heterobrochate. *Retibrevitricolporites yavarensis* (Hoorn 1993) Silva-Caminha et al. (2010) is micro-foveolate.

Stratigraphic range. T16.

Retibrevitricolporites? *toigoae* sp. nov.
Plate 7, figures 8–11

Holotype. 1AS-33-AM, 276 (3), EF: E33/4.

Paratype. 1AS-33-AM, 115 (6), EF: E23/3.

Etymology. After the Brazilian palynologist Marleni Toigo.

Diagnosis. Monad, mid-sized, tricolporate, brevicolpate, colpi slit-like, tectate, suprareticulate, homobrochate, pores lalongate, costate.

Description. Monad, amb circular; tricolporate; tectate, exine 2 μm thick, nexine 0.5 μm, columellae 0.5 μm visible under tectum, tectum 0.5 to 1 μm; sculpture suprareticulate, reticulum formed by muri on top of an entire tectum; homobrochate, lumina 1–2 μm wide, muri 1.5 μm wide; ectocolpi simple, ends pointed, thin, slit-like in equatorial view, 12 μm long; endopore costate, lalongate, 11 μm wide, 2–3 μm tall, costae 2 μm thick and 5 μm wide, wider at middle part of pore, thinning toward extremities of colpi.

Intraspecific variability. Aperture sometimes indistinct.

Dimensions. Equatorial view polar diameter 32 μm, equatorial diameter 40 μm (holotype); polar view diameter 41–(43.5)–45 μm long, 35–(40.7)–45 μm wide (paratype = 44 × 39 μm); nm = 5, no = 55.

Comparisons. *Retibrevitricolporites costaporus* sp. nov. is semitectate. *Bombacacidites araracuarensis* Hoorn 1994 is duplicolumellate. *Retibrevitricolporites protrudens* Legoux 1978 has strongly protruding apertures. *Retibrevitricolporites grandis* Jaramillo & Dilcher (2001) has fine reticulum and indistinct pores. *Retibrevitricolporites speciosus* Jaramillo & Dilcher (2001) is strongly heterobrochate. *Retibrevitricolporites yavarensis* (Hoorn 1993) Silva-Caminha et al. (2010) is micro-foveolate.

Stratigraphic range. T15–T16.

RHOIPITES Wodehouse 1933

Type species. *Rhoipites bradleyi* Wodehouse 1933.

Rhoipites alfredii sp. nov.
Plate 7, figures 12–16
Retitrescolpites sp. 1 Silva-Caminha et al. 2010, p. 64, Plate 7, figures 25–26.

Holotype. 1AS-33-AM, 239.90 m (1), EF: G41.

Paratype. 1AS-33-AM, 239.90 m (2), EF: H36/1.

Etymology. After the North American palynologist Alfred Traverse.

Diagnosis. Monad, mid-sized, tricolporate, semitectate, reticulate, heterobrochate, simplicolumellate, endopore circular, annulate.

Description. Monad pollen grain, amb circular; tricolporate; semitectate, exine 3.5 μm, nexine 1 μm, simplicolumellate, columellae 1 μm, tectum 1.5 μm; sculpture reticulate, heterobrochate, lumina 2–5 μm, muri 1.5 μm; foveolate at the poles, foveolae <1 μm, ectocolpi simple, pointed tips, 20 μm long, 12 μm wide; endopore annulate, circular 7 μm, annuli 2 μm wide.

Dimensions. Polar diameter 35–(40.8)–46 μm, equatorial diameter 45–(45.4)–46 μm (holotype = 45 × 35 μm, paratype = 46 × 38 μm, folded); nm = 5, no = 9.

Comparisons. *Rubipollis mulleri* Silva-Caminha et al. (2010) has lumina decreasing toward colpi. *Rhoipites cienaguensis* (Dueñas 1980) Barreda 1997, *R. squarrosus* (Van der Hammen & Wymstra 1964) Jaramillo & Dilcher (2001), *R. hispidus* (Van der Hammen & Wymstra 1964) Jaramillo & Dilcher, *R. baculatus* Archangelsky 1973, *R. pisinnus* Stanley 1965 and *R. nitidus* Sah & Dutta 1967 all have fine reticula. *Rhoipites planipolaris* Jaramillo et al. 2010 is foveolate at the apocolpia. *Rhoipites guianensis* (Van der Hammen & Wymstra 1964) Jaramillo & Dilcher (2001) has elongated lumina and bireticulate

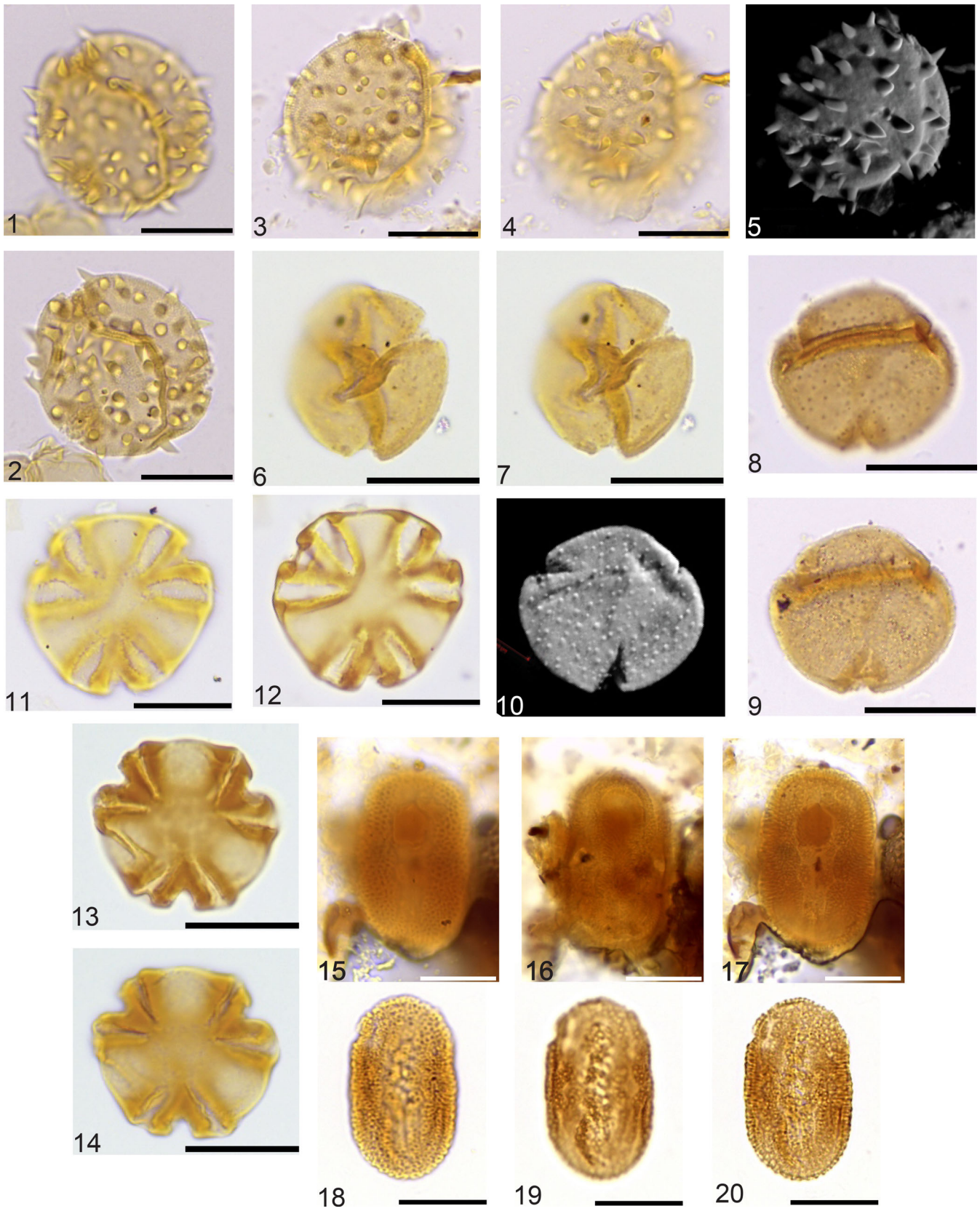

Plate 6. Figures 1, 2. *Malvacipolloides echibaculatus* sp. nov., holotype, 1AS-37-AM, 96.35 m (1), EF: T34/1-2. Figures 3, 4, 5. *Malvacipolloides echibaculatus* sp. nov. paratype, 1AS-37-AM, 34.90 m (2), EF: B33/C34. Figures 6, 7. *Malvacipolloides romeroae* sp. nov., holotype: AM27-22: Y70/1. Figures 8, 9, 10. *Malvacipolloides romeroae* sp. nov. paratype: 1AS-33-AM, 239.90 m (2), EF: D34. Figures 11, 12. *Margocolporites carinae* sp. nov., holotype, 1AS-33-AM, 77.10 m (6), EF: F48/2. Figures 13, 14. *Margocolporites carinae* sp. nov., paratype, 1AS-33-AM, 203.15 m (2), EF: H43-J. Figure 15, 16, 17. *Multiareolites*? *reticulatus* sp. nov., holotype, 1AS-33-AM, 186.60 m (2), EF: Q41/4-R. Figures 18, 19, 20. *Multiareolites*? *reticulatus* paratype: 1AS-33-AM, 203 (2): EF: H33. Scale bars: 20 μm.

ornamentation. *Rhoipites gigantoporus* Silva-Caminha et al. (2010) is homobrochate. *Rhoipites manausensis* D'Apolito et al. 2019 has a narrow and lalongate pore. *Rhoipites*? *perprolatus* Rodriguez et al. 2012 and *R.*? *basicus* D'Apolito et al. 2019 are tricolpate.

Stratigraphic range. T15–T16.

STEPHANOCOLPORATE

PSILASTEPHANOCOLPORITES Leidemeyer 1966

Type species. *Psilastephanocolporites fissilis* Leidelmeyer 1966.

Psilastephanocolporites deoliverae sp. nov.
Plate 7, figures 17–21

Holotype. 1AS-33-AM, 399.10 m (2), EF: U48/2-4.

Paratype. 1AS-33-AM, 77.10 m (6), EF: S48-49.

Etymology. After the Brazilian palynologist Paulo E. de Oliveira.

Diagnosis. Monad, mid-sized, 11 colporate, pores anastomosed, atectate, psilate, sometimes foveolate at poles.

Description. Monad, amb circular; stephanocolporate; atectate, exine 3 μm, sculpture psilate; sometimes foveolate at poles; ectocolpi simple, long, 11 colpi, pointed tips, 22 μm long, 2 μm wide; endopore simple, lalongate, 5 μm wide, 2 μm tall, pores almost anastomosing, but not forming endocingulum.

Dimensions. Equatorial view polar diameter 31–(31.3)–32 μm, equatorial diameter 28–(28.3)–29 μm (holotype = 32 × 29 μm); polar view diameter 42 μm long, 41 μm wide (paratype); nm = 4, no = 18.

Comparisons. *Psilastephanocolporites brevicolpatus* Jaramillo & Dilcher (2001) has 10–14 brevicolporate apertures. *Psilastephanocolporites fissilis* Leidelmeyer 1966 is endocingulate and only psilate. *Psilastephanocolporites brevicolpatus* Jaramillo & Dilcher (2001) has very short colpi.

Botanical affinity. Polygalaceae.

Stratigraphic range. T14–T16.

Psilastephanocolporites endoporatus sp. nov.
Plate 8, figures 1–4

Holotype. 1AS-33-AM, 320.25 m (1), EF: G35.

Paratype. 1AS-33-AM, 320.25 m (1), EF: V57.

Etymology. After the presence of endopores.

Diagnosis. Monad, 4–5-colporate, reticulate, mid-sized, tectate, psilate to microreticulate, granulose nexine at mesocolpia.

Description. Monad, prolate-spheroidal; stephanocolporate; 4–5 colporate, tectate, exine 4 μm, nexine 2 μm, columellae 1.5 μm, tectum 0.5 μm, sculpture varying from psilate to microreticulate; sometimes foveolate at poles; nexine thinner in the mesocolpia area, where it becomes granulose; ectocolpi simple, long, 17 μm long, 2 μm wide, ends pointed; endopore simple, circular, 3 μm wide.

Intraspecific variability. Sometimes the pore is annulate.

Dimensions. Polar diameter 28–(29)–31 μm, equatorial diameter 26–(27)–28 μm (holotype = 28 × 26 μm, paratype = 28 × 27 μm); nm = 3, no = 3.

Comparisons. *Psilastephanocolporites daportae* Herngreen 1975 is atectate. *Psilastephanocolporites laevigatus* Salard-Cheboldaeff 1978 is atectate, nexine thiner than the sexine, colpi costate. *Psilastephanocolporites brevissimus* D'Apolito et al. 2019 and *P. marinamensis* Hoorn 1994 have very short colpi. *Psilastephanocolporites brevicolpatus* Jaramillo & Dilcher (2001) has >10 short colpi. *Psilastephanocolporites fissilis* Leidelmeyer 1966 has more colpi and endocingulum. *Psilastephanocolporites globulus* van Hoeken-Klinkenberg 1966 is much smaller and intectate. *P. hoekenae* Herngreen 1975 has >7 colpi with concave sides. *Psilastephanocolporites matapiorum* Hoorn 1994 has a different shape and costate colpi. *Psilastephanocolporites punctatus* Salard-Cheboldaeff 1978 has short colpi and a subrectangular shape. *Psilastephanocolporites variabilis* Regali et al. 1974 has >5 short colpi and straight sides in polar view. *Psilastephanocolporites schneideri* Hoorn (1993) has much smaller and lalongate pores. *Psilastephanocolporites perforatus* Salard-Cheboldaeff 1978 has lalongate costate pores.

Stratigraphic range. T15.

RETISTEPHANOCOLPORITES van der Hammen & Wymstra 1964

Type species. *Retistephanocolporites quadriporus* Van der Hammen & Wymstra 1964.

Retistephanocolporites elizabeteae sp. nov.
Plate 8, figures 5–8

Holotype. 1AS-33-AM 399.10 m (1), EF: Q34/1.

Paratype. 1AS-33-AM 399.10 m (1), EF: R37/4.

Etymology. After the Brazilian palynologist Elizabete Pedrão Ferreira.

Diagnosis. Monad, 5-colporate, reticulate, heterobrochate, lumina wider at apocolpia, microreticulate in mesocolpia.

Description. Monad, amb circular; stephanocolporate; 5-colporate, semi-tectate, exine 2 μm, tectum 0.5 μm, columella, 0.5 μm, nexine 1 μm, sculpture reticulate; strongly heterobrochate, reticulum wider at apocolpia and decreases toward mesocolpia, where it is microreticulate; lumina in apocolpium is 3 to 8 μm long and abruptly changes to microreticulum <1 μm in mesocolpium; ectocolpi 16 μm long, 6 μm wide, marginate, margo 3 μm wide and decreasing toward tips of colpi, margo formed by reticulum that decreases in size around colpi, ends of colpi pointed, endopores slightly annulate, annulus 2 μm wide and 1.5 μm thick, circular, 5 μm across.

Dimensions. Polar view diameter 46–(47)–48 μm long, 44–(46)–48 μm wide (holotype = 48 × 48 μm, paratype = 46 × 44 μm); nm = 2, no = 2.

Comparisons. *Retistephanocolporites festivus* Gonzalez 1967 has uniform lumina. *Retistephanocolporites centrimaculatus* D'Apolito et al. (2019) is smaller (25 μm). *Jandufouria minor* Jaramillo & Dilcher (2001) is microreticulate and homobrochate. *Retistephanocolporites fossulatus* Jaramillo & Dilcher (2001) is 4-colporate and fossulate-reticulate-foveolate.

Stratigraphic range. T14.

Botanical affinity. *Ceiba* (Malvaceae).

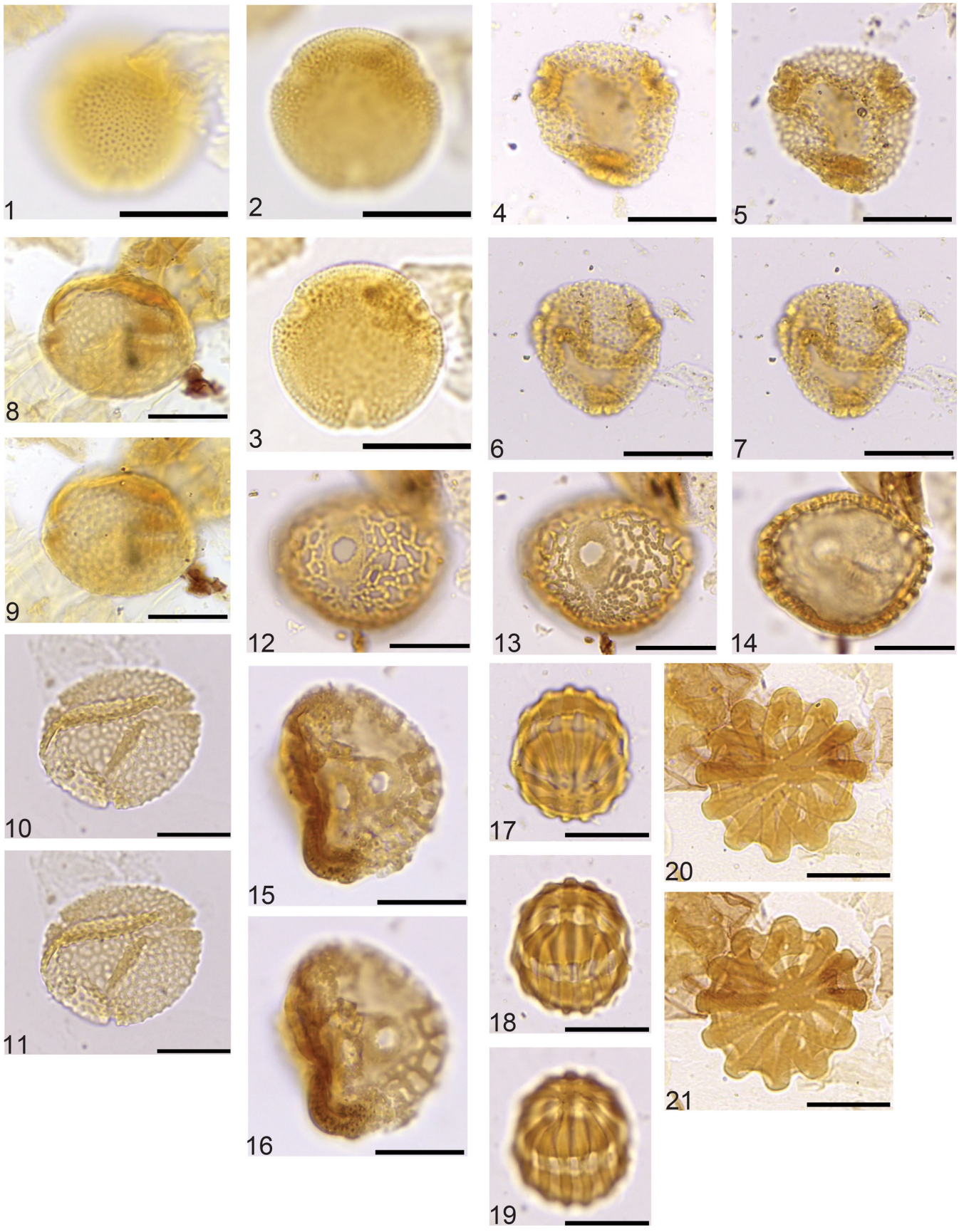

Plate 7. Figures 1, 2, 3. *Ranunculacidites reticulatus* sp. nov., holotype, 1AS-37-AM, 96.65 m (2), EF: S35/2. Figures 4, 5: *Retibrevitricolporites costaporus* sp. nov., holotype, 1AS-33-AM, 158.20 m (1), EF: G 54. Figures 6, 7: *Retibrevitricolporites costaporus* sp. nov., paratype, 1AS-33-AM, 158.20 m (1), EF: H49. Figures 8, 9. *Retibrevitricolporites*? *toigoae* sp. nov., holotype, 1AS-33-AM, 276 (3), EF: E33/4. Figures 10, 11. *Retibrevitricolporites*? *toigoae* sp. nov., paratype, 1AS-33-AM, 115 (6), EF: E23/3. Figure 11, 12, 13. *Rhoipites alfredii* sp. nov., holotype, 1AS-33-AM, 239.90 m (1), EF: G41. Figures 15, 16. *Rhoipites alfredii* sp. nov., paratype, 1AS-33-AM, 239.90 m (2), EF: H36/1. Figures 17, 18, 19. *Psilastephanocolporites deoliverae* sp. nov., holotype, 1AS-33-AM, 399.10 m (2), EF: U48/2-4. Figures 20, 21. *Psilastephanocolporites deoliverae* sp. nov., paratype, 1AS-33-AM, 77.10 m (6), EF: S48–49. Scale bars: 20 μm.

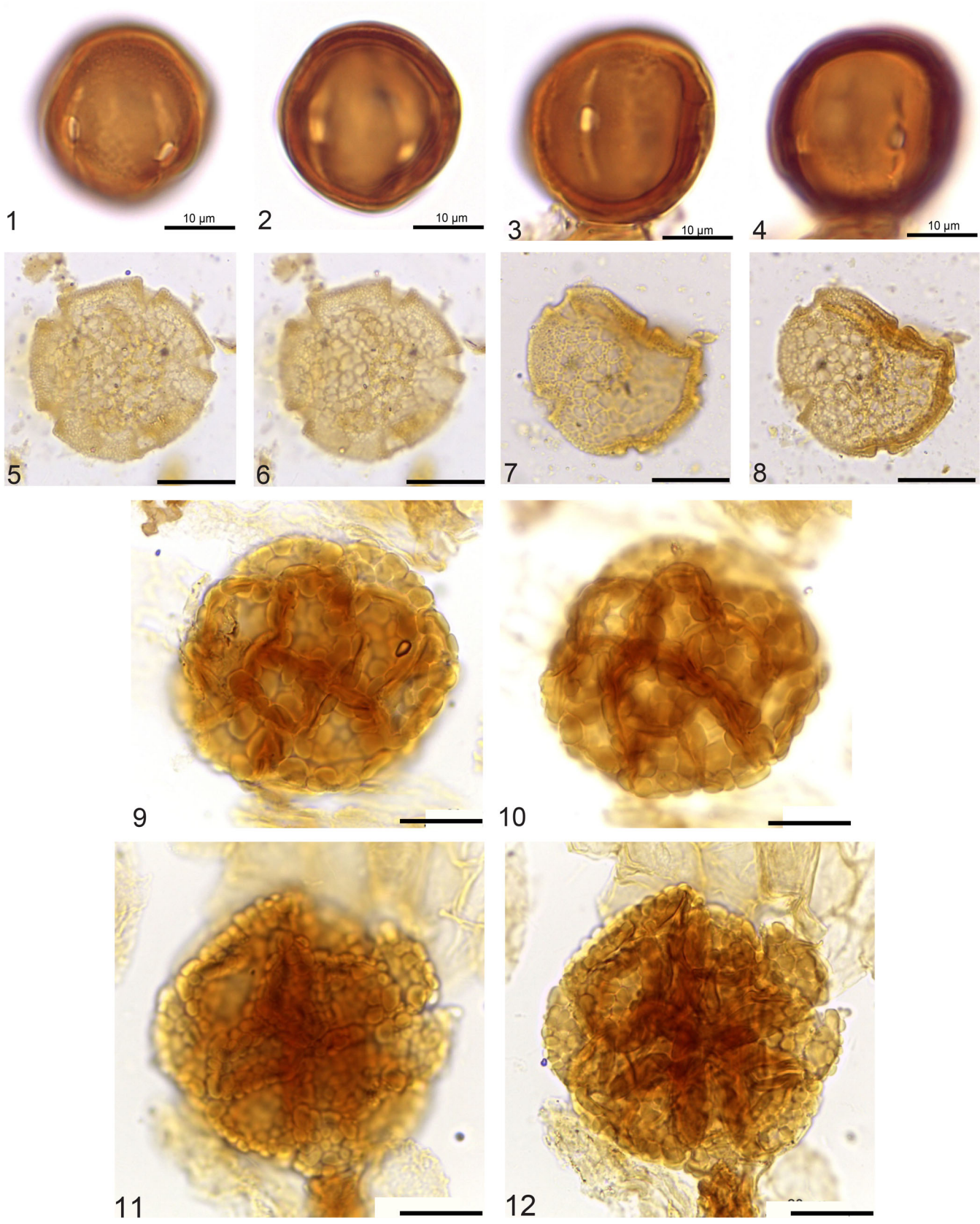

Plate 8. Figures 1, 2. *Psilastephanocolporites endoporatus* sp. nov., holotype, 1AS-33-AM, 320.25 m (1), EF: G35. Figures 3, 4. *Psilastephanocolporites endoporatus* sp. nov., paratype, 1AS-33-AM, 320.25 m (1), EF: V57. Figures 5, 6. *Retistephanocolporites elizabeteae* sp. nov., holotype, 1AS-33-AM 399.10 m (1), EF: Q34/1. Figures 7, 8. *Retistephanocolporites elizabeteae* sp. nov., paratype, 1AS-33-AM 399.10 m (1), EF: R37/4. Figures 9, 10. *Parkiidites marileae* sp. nov., holotype, 1AS-33-AM, 232.18 m (1), EF: J35/2. Figures 11, 12. *Parkiidites marileae* sp. nov., paratype, 1AS-33-AM, 232.18 m (1), EF: K29/3. Scale bars: 20 µm.

POLYAD

PARKIIDITES Guinet & Salard-Cheboldaeff 1975

Type species. *Parkiidites microreticulatus* Guinet & Salard-Cheboldaeff 1975.

Parkiidites marileae sp. nov.
Plate 8, figures 9–12

Holotype. 1AS-33-AM, 232.18 m (1), EF: J35/2.
Paratype. 1AS-33-AM, 232.18 m (1), EF: K29/3.
Etymology. After the Brazilian palynologist Maria Lea Salgado-Labouriau.
Diagnosis. Polyad, 16 monads, intectate, large-sized, verrucate.
Description. Polyad, formed by 16 monads, arranged in 4 monads proximally, 4 distally and 8 monads around them; polyad circular, monads shape not clear, apparently of irregular shape; exine intectate, densely verrucate, verrucae vary in size and shape, 3–7 μm long; 3 μm tall, 0.5 μm apart, rounded to oval, nexine 1 μm thick; monad 20–28 μm.
Dimensions. Polyad diameter 60–(69.8)–74 μm long, 50–(60.2)–71 μm wide (holotype = 70 × 62 μm, paratype = 74 × 71 μm); nm = 5, no = 11.
Comparisons. *Polyadopollenites mariae* Dueñas 1980 and *Acaciapollenites myriosporites* (Cookson 1954) Mildenhall 1972 have 16 monads and are psilate. *Polyadopollenites vancampoi* Salard-Cheboldaeff 1978 also has 16 monads and it is smaller (40–65 μm). *Parkiidites macroreticulatus* Salard-Cheboldaeff 1974 is reticulate.
Botanical affinity. *Parkia* (Fabaceae).
Stratigraphic range. T16.

6. Concluding remarks

In the present contribution we studied the systematic palynology of two boreholes (1-AS-33-AM and 1-AS-37-AM) from the Solimões Formation in western Amazonia. We found the following sequence of events: the FAD of *Multimarginites vanderhammeni*, *Crassoretitriletes vanraadshoovenii*, *Fenestrites spinosus* and *Paleosantalaceapites cingulatus*; the FCO of *Grimsdalea magnaclavata*; followed by the first appearance of *Cichoreacidites longispinosus* and *Echitricolporites mcneillyi*. We applied the Colombian and Venezuelan zonation schemes in order to date both cores. The age of core 33AM (404.5 m) established by Leite et al. (2017) was revised and repositioned in the early middle Miocene to late Miocene, corresponding to zones T14 (~16–14.2 Ma), T15 (14.2–12.7 Ma), and T16 (12.7–7.1 Ma) of Jaramillo et al. (2011). Core 37AM (242.6 m) was correlated to core 33AM; it is placed almost entirely in zone T16. The basal ~40 m had no pollen samples, but by extrapolation it could correspond to zone T15. We also revised and increased pollen counts of an outcrop in the Acre Basin, the Patos section, where we found *Cyatheacidites annulatus* co-occurring with *Echitricolporites mcneillyi* for the first time. The record of *C. annulatus* indicates an age around 7 Ma or younger for the outcrop. The widespread occurrence of *Cyatheacidites annulatus* in outcrops of the Solimões Formation indicates the existence of latest Miocene (~7 Ma) to Pliocene sedimentation and an age older than ~7 Ma for the uppermost sediments of boreholes. Biostratigraphic relationships also indicate that *Echitricolporites mcneillyi* and *Ladakhipollenites*? *caribbiensis* cannot be used as Pliocene markers as previously assigned.

Acknowledgements

FPRL thanks Coordenação de Aperfeiçoamento de Pessoal em Nível Superior (CAPES) for a postdoctoral scholarship (PNPD-CAPES). CD thanks Conselho Nacional de Ciência e Tecnologia (CNPq) and Fundação de Amparo à Pesquisa do Estado de Mato Grosso (FAPEMAT) for a research grant (568838/2017). SAFSC thanks CNPq for a research grant (476020/2013-1). We are grateful to Karina E. Kachniasz for help with pollen counts from Patos and to PETROBRAS/CENPES/PDEP/BPA (Gerência de Bioestratigrafia e Paleoecologia), Elizabete Pedrão Ferreira, and Andrea Wallau Souto-Ribeiro for confocal images. We are indebted to the editor James Riding, Carlos Jaramillo, and an anonymous reviewer for their helpful comments.

Disclosure statement

The authors have no potential conflict of interest to report.

Author contributions

FPRL processed samples, counted pollen slides, and wrote the initial draft; all authors were involved in pollen description and identification, and in writing and revision of the final manuscript.

Funding

This work was supported by the Coordenação de Aperfeiçoamento de Pessoal em Nível Superior (CAPES); Conselho Nacional de Desenvolvimento Científico e Tecnológico (CNPq) and Fundação de Amparo à Pesquisa do Estado de Mato Grosso (FAPEMAT) [grant 568838/2017]; and CNPq [grant 476020/2013-1].

Notes on contributors

FATIMA PRAXEDES RABELO LEITE earned her bachelor's degree in biology from the Universidade Santa Ursula in 1990 and her master's degree in sedimentary geology, awarded by the Universidade de São Paulo in 1997. Fatima then obtained a PhD in Geology from the Universidade Federal de Brasília in 2006. She has undertaken three postdoctoral contracts at the Smithsonian Tropical Research Institute, Panama in 2007 and 2010/2011 and Universidade Federal de Mato Grosso 2014-2018. Fatima's research is on the Neogene biostratigraphy, paleoecology and palynology of Amazonia.

SILANE A. F. DA SILVA CAMINHA is a lecturer at the Universidade Federal de Mato Grosso, Brazil. Her main reaseach interests are Neogene pollen analysis, paleoecology and pollen morphology, especially the origin and evolution of the Amazon and Pantanal.

CARLOS D'APOLITO is a postdoctoral researcher at the Universidade Federal de Mato Grosso (UFMT) in Cuiaba, Brazil. His main research interests are the evolution of vegetation and landscapes, palynology, palynostratigraphy and paleobiogeography in neotropical areas during the Mesozoic and Cenozoic.

ORCID

Silane Aparecida Ferreira da Silva-Caminha https://orcid.org/0000-0003-4853-2789
Carlos D'Apolito https://orcid.org/0000-0003-1602-0201

References

Al-Hakimi AS, Maideen H, Saeed AA, Faridah QZ, Latiff A. 2017. Pollen and seed morphology of Justicieae (Ruellioideae, Acanthaceae) of Yemen. Flora. 233:31–50.

Backman J, Raffi I, Rio D, Fornaciari E, Pälike H. 2012. Biozonation and biochronology of Miocene through Pleistocene calcareous nannofossils from low and middle latitudes. Newsletters on Stratigraphy. 45(3): 221–244.

Bissaro-Júnior MC, Kerber L, Crowley JL, Ribeiro AM, Ghilardi RP, Guilherme E, Negri FN, Souza Filho JP, Hsiou AS. 2019. Detrital zircon U-Pb geochronology constrains the age of Brazilian Neogene deposits from Western Amazonia. Palaeogeography Palaeoclimatology Palaeoecology. 516:64–70.

Boonstra M, Ramos MIF, Lammertsma EI, Antoine PO, Hoorn C. 2015. Marine connections of Amazonia: evidence from foraminifera and dinoflagellate cysts (early to middle Miocene, Colombia/Peru). Palaeogeography Palaeoclimatology Palaeoecology. 417:176–194.

Boudagher-Fadel MK. 2015. Biostratigraphic and geological significance of Planktonic Foraminifera. London (UK): UCL Press; 310 p.

Campbell KE, Jr., Frailey CD, Romero-Pittman L. 2006. The Pan-Amazonian Ucayali Peneplain, late Neogene sedimentation in Amazonia, and the birth of the modern Amazon River system. Palaeogeography Palaeoclimatology Palaeoecology. 239(1–2):166–219.

Caputo MV. 1984. Stratigraphy, tectonics, paleoclimatology and paleogeography of Northern Basins of Brazil [Doctoral thesis]. Santa Barbara, CA: California University.

Cozzuol MA. 2006. The Acre vertebrate fauna: Age, diversity, and geography. Journal of South American Earth Sciences. 21(3):185–203.

Cunha P. 2007. Bacia do Acre. Boletim de Geociencias - Petrobras, Rio De Janeiro. 15 (2):207–215.

D'Apolito C, da Silva-Caminha SAF, Jaramillo C, Dino R, Soares EAA. 2019. The Pliocene–Pleistocene palynology of the Negro River, Brazil, Palynology. Palynology. 43(2):223–243.

Eiras JF, Becker CR, Souza EM, Gonzaga JEF, Silva LM, Daniel LMF, Matsuda NS, Feijó FJ. 1994. Bacia do Solimões. Boletim de Geociencias - Petrobras, Rio De Janeiro. 8 (1):17–45.

Espinosa BS, D'Apolito C, Silva-Caminha SAF, Ferreira MG, Absy ML. 2020. Neogene paleoecology and biogeography of a Malvoid pollen in northwestern South America. Review of Palaeobotany and Palynology. 273:104131.

Foote M. 2000. Origination and extinction components of taxonomic diversity: general problems. In: Erwin DH, Wing SL, editors. Deep time: Paleobiology's perspective. Chicago, IL: The Paleontological Society; p. 74–102.

Germeraad JH, Hopping CA, Muller J. 1968. Palynology of Tertiary sediments from tropical areas. Review of Palaeobotany and Palynology. 6(3–4):189–348.

Gomes BT, Absy ML, D'Apolito C, Jaramillo C, Almeida R. 2019. Compositional and diversity comparisons between the palynological records of the Neogene (Solimões Formation) and Holocene sediments of western Amazonia. Palynology.

Gross M, Piller WE, Ramos MI, Silva-Paz JD. 2011. Late Miocene sedimentary environments in south-western Amazonia (Solimões Formation; Brazil). Journal of South American Earth Sciences. 32(2):169–181.

Hoorn C, Bogotá-A GR, Romero-Baez M, Lammertsma EI, Flantua SGA, Dantas E, Dino R, Carmo DA, Chemale JF. 2017. Amazon at sea: Onset and stages of the Amazon River from a marine record, with special reference to Neogene plant turnover in the drainage basin. Global and Planetary Change. 153:51–65.

Hoorn C, Wesselingh FP, ter Steege H, Bermudez MA, Mora A, Sevink J, Sanmartin I, Sanchez-Meseguer A, Anderson CL, Figueiredo JP, et al. 2010. Amazonia through time: Andean uplift, climate change, landscape evolution and biodiversity. Science. 330(6006):927–931.

Hoorn C. 1993. Marine incursions and the influence of Andean tectonics on the Miocene depositional history of northwestern Amazonia: results of a palynostratigraphic study. Palaeogeography Palaeoclimatology Palaeoecology. 105(3–4):267–309.

Horbe AMC, Roddaz M, Gomes LB, Castro RT, Dantas EL, Carmo DA. 2019. Provenance of the Neogene sediments from the Solimões Formation (Solimões and Acre Basins), Brazil. Journal of South American Earth Sciences. 93:232–241.

Jaramillo C, Dilcher DL. 2001. Middle Paleogene palynology of Central Colombia, South America: a study of pollen and spores from tropical latitudes. Palaeontographica Abteilung B. 258(4–6):87–213.

Jaramillo C, Romero I, D'Apolito C, Bayona G, Duarte E, Louwye S, Escobar J, Luque J, Carrillo-Briceño JD, Zapata V, et al. 2017. Miocene flooding events of western Amazonia. Science Advances. 3(5): e1601693.

Jaramillo C, Rueda M, Torres V. 2011. A palynological zonation for the Cenozoic of the Llanos and Llanos Foothills of Colombia. Palynology. 35(1):46–84.

Jaramillo C, Rueda MJ. 2020. A morphological electronic database of Cretaceous-Tertiary and extant pollen and spores from Northern South America, v. 2020. Available from: http://biogeodb.stri.si.edu/jaramillosdb/web/morphological/.

Jorge V, D'Apolito C, da Silva-Caminha SAF. 2019. Exploring geophysical and palynological proxies for paleoenvironmental reconstructions in the Miocene of western Amazonia (Solimões Formation, Brazil). Journal of South American Earth Sciences. 94:102223.

Kachniasz KE, Silva-Caminha S. 2017. Palinoestratigrafia da Formação Solimões: comparação entre bioestratigrafia tradicional e o método de Associações Unitárias. Revista Brasileira de Paleontologia. 19(3): 481–490.

Latrubesse E, Silva SF, Cozzuol M, Absy ML. 2007. Late Miocene continental sedimentation in the southwestern Amazonia and its regional significance: Biotic and geological evidence. Journal of South American Earth Sciences. 23(1):61–80.

Latrubesse EM, Cozzuol M, Silva-Caminha SAF, Rigsby CA, Absy ML, Jaramillo C. 2010. The late Miocene paleogeography of the Amazon basin and the evolution of the Amazon River system. Earth-Science Reviews. 99(3–4):99–124.

Leandro LM, Vieira CEL, Santos A, Fauth G. 2019. Palynostratigraphy of two Neogene boreholes from the northwestern portion of the Solimões Basin, Brazil. Journal of South American Earth Sciences. 89: 211–218.

Leite FPR, Paz JD, Do Carmo DA, Silva-Caminha S. 2017. The effects of the inception of Amazonian transcontinental drainage during the Neogene on the landscape and vegetation of the Solimões Basin, Brazil. Palynology. 41(3):412–422.

Linhares AP, Gaia VCS, Ramos M. 2017. The significance of marine microfossils for paleoenvironmental reconstruction of the Solimões Formation (Miocene), western Amazonia, Brazil. Journal of South American Earth Sciences. 79:57–66.

Linhares AP, Ramos MIF, Gaia VCS, Friaes YS. 2019. Integrated biozonation based on palynology and ostracods from the Neogene of Solimões Basin, Brazil. Journal of South American Earth Sciences. 91: 57–70.

Linhares AP, Ramos MIF, Gross M, Piller WE. 2011. Evidence for marine influx during the Miocene in southwestern Amazonia, Brazil. Geología Colombiana. 36(1):91–104.

Lorente MA. 1986. Palynology and palynofacies of the Upper Tertiary in Venezuela. Dissertatione Botanicae, Band 99. Berlin: Lubrecht & Cramer Ltd.

Maia RG, Godoy HK, Yamaguti HS, Moura PA, Costa FS, Holanda MA, Costa J. 1977. Projeto de carvão no Alto Solimões: Relatório final. Manaus: CPRM-DNPM; 137p.

Medeiros CG, Carmo DA, Antonietto LS, Boush L. 2019. The ostracods from Solimões Formation, Brazil: an alternative biostratigraphic zonation for the neogene of Amazonia. Revista Brasileira de Paleontologia. 22(2):97–105.

Medeiros CG, Carmo DA, Antonietto LS, Graça MC. 2017. Identificação de evento paleoambiental no Mioceno da Amazônia Ocidental, Formação Solimões. In: Simpósio de Geologia da Amazônia. Belém (Brazil): SBG-Núcleo Norte; pp. 790–793.

Muller J, Giacomo E, Van Erve AW. 1987. A palynological zonation for the Cretaceous, Tertiary and Quaternary of Northern South America. American Association Stratigraphic Palynologists, Contribution Series. 19:7–76.

Nogueira ACR, Silveira RR, Guimarães J. 2013. Neogene-Quaternary sedimentary and paleovegetation history of eastern Solimões Basin, Central Amazon region. Journal of South American Earth Sciences. 46:89–99.

Ortiz J, Jaramillo C. 2019. SDAR: stratigraphic data analysis. R Package Version 0.9-3. Available from: https://CRAN.R-project.org/package=SDAR.

Punt W, Hoen PP, Blackmore S, Nilsson S, Le Thomas A. 2007. Glossary of pollen and spore terminology. Review of Palaeobotany and Palynology. 143(1–2):1–81.

R Core Team. 2018. R: a language and environment for statistical computing. R Foundation for Statistical Computing, Vienna. Available from: https://www.R-project.org.

Sá NP, Carvalho MA, Correia GC. 2020. Miocene paleoenvironmental changes in the Solimões Basin, western Amazon, Brazil: A reconstruction based on palynofacies analysis. Palaeogeography Palaeoclimatology Palaeoecology. 537.

Salamanca S, Van Soelen EE, Van Manen MT, Flantua S, Santos RV, Roddaz M, Dantas EL, van Loon E, Damsté JS, Kim JH, et al. 2016. Amazon forest dynamics under changing abiotic conditions in the early Miocene. (Colombian Amazonia). Journal of Biogeography. 43(12):2424–2437.

Silva-Caminha SAF, Jaramillo C, Absy ML. 2010. Neogene palynology of the Solimões Basin, Brazilian Amazonia. Palaeontographica Abteilung B. 284 (1–3):13–67.

Silveira RR, Souza PA. 2015. Palinologia (grãos de pólen de angiospermas) das formações Solimões e Içá (bacia do Solimões), nas regiões de Coari e Alto Solimões, Amazonas. Revista Brasileira de Paleontologia. 18(3):455–474.

Sundell KE, Saylor JE, Lapen TJ, Horton BK. 2019. Implications of variable late Cenozoic surface uplift across the Peruvian central Andes. Scientific Reports. 9(1):4877.

Turland NJ, Wiersema JH, Barrie FR, Greuter W, Hawksworth DL, Herendeen PS, Knapp S, Kusber W-H, Li D-Z, Marhold K, et al. 2018. International Code of Nomenclature for algae, fungi, and plants (Shenzhen Code) adopted by the Nineteenth International Botanical Congress Shenzhen, China. Regnum Vegetabile 159. Glashütten: Koeltz Botanical Books.

Wesselingh FP, Räsänen ME, Irion G, Vonhof HB, Kaandorp R, Renema W, Romero Pittman L, Gingras M. 2002. Lake Pebas: a palaeoecological reconstruction of a Miocene, long-lived lake complex in western Amazonia. Cainozoic Research. 1:35–81.